



MONASH University
Engineering

Smart Antenna Beamforming for Remote Sensing

ENG4702: Final Year Project - Final Report

Author(s): Alexander Li (30630711)

Student ID(s): 30630711

Supervisor(s): Emanuele Viterbo

Date of Submission: 26 May 2025

Project type: Research

1 Executive Summary

Phased array antennas are critical to modern wireless systems, enabling high-speed communication, radar, and satellite remote sensing. To reduce cost and power consumption, many systems use low-resolution digital phase shifters. However, these components are vulnerable to bit-level hardware faults - where individual bits in the digital control signal become permanently stuck. Such faults degrade the beamforming accuracy of the antenna, potentially impairing system performance.

This project aimed to develop a fault-aware beamforming method that compensates for bit-level faults in digital phase shifters, without requiring hardware redundancy. A novel fault model was introduced to represent scenarios where some bits in a phase shifter fail while others remain functional - a case not addressed in existing literature. To address this, an Element-wise Local Optimisation (ELO) algorithm was designed to quickly and effectively recover the antenna's radiation pattern by adjusting only the working bits of each phase shifter.

The algorithm was evaluated through simulation using Monte Carlo trials over all fault scenarios. Results showed that the ELO method achieved near-optimal beamforming recovery in real time, particularly in low-fault regimes that are common in practical applications. Standard optimisation methods - Genetic Algorithms (GA) and Binary Particle Swarm Optimisation (PSO), were adapted to this setting, and compared against ELO. The ELO algorithm performed competitively in terms of accuracy and significantly outperformed them in computational efficiency.

The major outcome of this work is a lightweight, fault-tolerant beamforming strategy that can extend the operational life and robustness of phased array systems using low-cost hardware. While the findings were validated in simulation, the method lays the groundwork for future implementation in real antenna systems, with potential applications in defence, telecommunications, and satellite remote sensing.

2 Acknowledgement of Country

I would like to acknowledge the traditional owners of the land on which I study and work, the Wurundjeri People of the Kulin Nations. I pay my respects to their Elders, past, present, and emerging, and recognise their continuing connection to land, waters, and culture. I extend that respect to all Aboriginal and Torres Strait Islander peoples. I acknowledge the contributions that Indigenous Australians have made to knowledge, technology, and innovation, and I am committed to fostering a respectful and inclusive environment in my work as an engineering student.

Contents

1 Executive Summary	2
2 Acknowledgement of Country	3
3 Introduction	5
4 Aims and Objectives	6
4.1 Research Question	6
4.2 Aims	6
4.3 Objectives	6
5 Literature Review	7
5.1 Beamforming with Planar Phased Array Antennas	7
5.2 Phase Shifter Technologies and Their Fault Scenarios	8
5.3 Fault Models	10
5.4 Beamforming Algorithm Optimisation Techniques	11
5.5 Research Gap	13
6 Methodology and Methods	14
6.1 Methodology	14
6.1.1 System Model - Ideal Beamforming	14
6.1.2 System Model - Quantised phase shifters	14
6.2 Method	15
6.2.1 Physical Antenna Array Inspection	15
6.2.2 Bit-level Fault Model Construction	16
6.2.3 Simulation of Quantisation and Bit-level Faults	16
6.2.4 Designing Element-wise Local Optimisation (ELO) algorithm	17
6.2.5 Implementing GA and BPSO	17
6.2.6 Monte Carlo Simulations of the Optimisation Algorithms	17
7 Results and Discussion	18
7.1 A Mathematical Model for Bit-level Faults	18
7.2 Simulation of Quantisation and Bit-level Faults	18
7.3 The ELO Algorithm and its Performance	20
7.4 The Performance of GA and BPSO	22
7.5 Monte Carlo Simulations	26
7.6 Summary of Findings	29
7.7 Limitations and Future Work	29
7.7.1 Simulation-Based Evaluation and Lack of Hardware Demonstration	29
7.7.2 Fixed Monte Carlo Sampling Budget	29
7.7.3 Absence of Statistical Failure Data for Phase Shifter Bits	30
7.7.4 Future Work	30
8 Conclusion	31
9 Reflection on Project Management	32
9.1 Project Scope	32
9.2 Project Plan & Timeline	32
9.2.1 Phase 1: Literature Review and Experimental Fault diagnosis - 9 weeks	32
9.2.2 Phase 2: Measurement of the Radiation Characteristics - 4 weeks	32
9.2.3 Phase 3: Repairing the Antenna- 7 weeks	32

9.2.4 Phase 4: Pivot and Novel Fault Model Identification - 5 weeks	32
9.2.5 Phase 5: Simulation and Data Collection - 3 weeks	32
9.2.6 Phase 6: Analysis and Comparison against baselines - 3 weeks	32
9.3 Reflection on Project	34
10 References	35
11 Appendices	38
11.1 Appendix A: Project Risk Assessment	38
11.2 Appendix B: Risk Management Plan	40
11.2.1 Major Activities	40
11.2.2 Health Concerns	40
11.2.3 Public Concerns	40
11.2.4 Risk Assessments	40
11.3 Appendix C: Sustainability Plan	42
11.3.1 SDG 6: Clean Water and Sanitation	42
11.3.2 Stakeholders	42
11.3.3 Positive Environmental Impact	42
11.3.4 Negative Environmental Impact and Mitigation	42
11.3.5 Resource Efficiency and Sustainable Design	42
11.3.6 Social Impact	42
11.3.7 Economic Impact	43
11.3.8 Summary	43
11.4 Appendix D: Generative AI Statement	43

3 Introduction

Phased array antennas have emerged as pivotal tools in modern radar and remote sensing systems, offering unprecedented capabilities for real-time environmental monitoring and data collection [1]. These systems operate by applying phase shifts to individual antenna elements that combine to form an array, creating constructive and destructive interference that reshape the radiation pattern into beams focused toward desired directions with high gain and precise control. This allows sensors to scan vast areas from afar with no complex mechanical dynamics. The ability to steer beams electronically without physically moving the array enhances system responsiveness and reliability, which is crucial in a wide range of applications including weather forecasting, earth observation, surveillance, and environmental monitoring such as soil moisture mapping [2, 3].

Beamforming is most widely implemented with electronic phase shifters (as opposed to mechanical or MEMS types), due to their CMOS compatibility, compact size and simple design [4]. The digital variant of electronic phase shifters involve changing the effective path length of the RF signal in discrete steps, with an associated bit resolution. Bit-level faults - when the physical component associated with each bit of the phase shifter becomes damaged, leading to those bits being uncontrollable and stuck at 0 or 1 - are a real fault encountered experimentally with such phase shifters. This leads to degradation of the radiation pattern, decreased gain, and increased sidelobes. Mitigation must be performed on the algorithmic level, for complex arrays where hardware redundancy is costly or impractical.

Despite their practical significance, the effects of bit-level phase shifter faults on beamforming performance are not addressed in current literature. The fault models considered in the current literature include element drop-out (where entire phase shifters and their corresponding elements fail and stop radiating), random phase offsets (added to a still-controllable phase), total phase shifter failure (where the entire phase shifter is stuck at a random phase), or deformations in the antenna leading to pattern-level degradations [5]. None address the bit-level faults that lead to partially-controllable phase shifters. Moreover, most conventional efforts to repair the beamforming performance utilise time-consuming optimisation algorithms such as the Genetic Algorithm (GA) [6] and the Particle Swarm Optimisation (PSO) [7], which are often unrealistic in deployed systems.

This project addresses this gap by investigating the impact of bit-level faults in digital electronic phase shifters and proposing algorithmic solutions to mitigate their effects. Specifically, it introduces an Element-wise Local Optimisation (ELO) technique that compensates for faulty phase states by minimizing deviation from the target phase in the binary-word space. Unlike conventional global optimisation approaches, the proposed method leverages knowledge of individual fault characteristics to improve radiation performance under hardware-imposed constraints to reach near-optimal performance and is fast enough to run in real time. The bit-level fault model is identified from a physical antenna provided by the “Airborne Passive Radiometer for High Resolution Soil Moisture Monitoring” (DP160104233) project of the Australian Research Council, and the beamforming algorithm’s ability to repair the radiation pattern was verified with simulation.

This work exists within the broader context of remote sensing and radar technology, particularly within ongoing efforts to develop multi-band, shared-aperture phased array systems for environmental monitoring applications. By improving fault tolerance in beamforming, this research supports the reliability and robustness of such systems, especially in mission-critical contexts where partial hardware failure must not compromise functionality. In doing so, this project contributes to both the theoretical understanding and practical implementation of resilient phased array systems - a step toward more robust, scalable, and fault-aware beamforming in real-world sensing applications.

4 Aims and Objectives

4.1 Research Question

How can the performance of a phased array antenna be affected when low-resolution digital phase shifters suffer from bit-level faults, and what algorithmic strategies can mitigate the impact of these hardware constraints?

4.2 Aims

To develop and evaluate a fault-aware beamforming approach that compensates for bit-level faults in phase shifters, improving the radiation pattern of phased array antennas without requiring hardware redundancy.

4.3 Objectives

1. **Model bit-level faults in phased array systems.** Develop a mathematical framework that captures the behaviour of phased arrays with faulty phase shifter bits.
2. **Design a beamforming optimisation algorithm.** Implement an element-wise optimisation method that achieves near optimal performance for reasonable fault states and can run in real time.
3. **Simulate and evaluate performance.** Validate the proposed algorithm through simulation, evaluating its radiation pattern accuracy, peak side-lobe level, and peak beam power. Compare against the baseline solutions in the literature - GA and PSO.
4. **Assess practical implications and limitations.** Discuss the algorithm's applicability to different phase shifter technologies, and scalability.

5 Literature Review

5.1 Beamforming with Planar Phased Array Antennas

The principles of beamforming with planar phased array antennas are included here to establish a theoretical foundation for the rest of the report.

Beamforming is the conversion of an isotropic radiation pattern into one that has high directivity along an axis that can be steered utilising wave interference, achieved by phase shifting a multi-element array of smaller antennas, shown in Figure 1. This provides a three-fold benefit of higher gain, finer spatial resolution, and higher area coverage by beam steering, making it ideal for satellite applications [8].

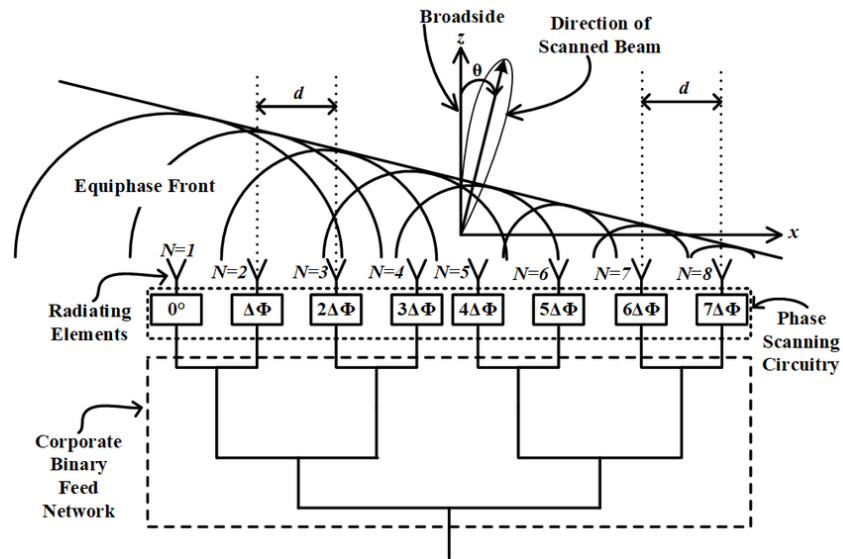


Figure 1: A typical phased array antenna. A binary feed network delivers power to the network while ensuring uniform path length up to the phase shifters across all elements. The phase shifters delay the radiation of the elements by a progressive phase, causing the resultant wavefronts to travel in a controlled direction [9].

While the wavefront picture in Figure 1 presents a simple intuition for beamforming and beam-steering, the actual radiation pattern is more complex, and requires a deeper theoretical treatment. Fourier optics reveals that the far-field radiation pattern is the Fourier Transform of the radiating elements' aperture function [10, 11]. Thus the rectangular array of square grids should result in a large Fraunhofer pattern enveloping a multi-slit interference pattern. There will be a central spot where most of the intensity is concentrated (hence the increased directivity), along with unavoidable side lobes mainly along the dimensions of the rectangular array. This pattern is shown in Figure 2.

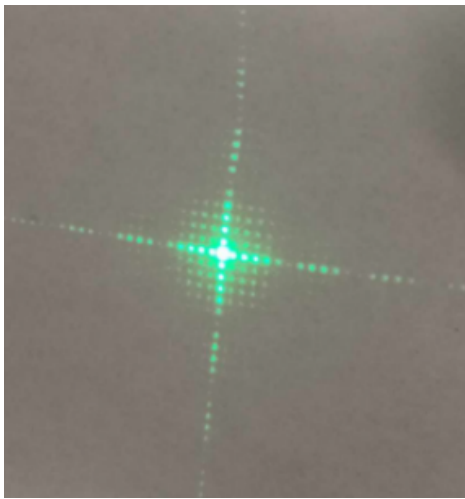


Figure 2: A typical transverse radiation pattern produced by a planar array.

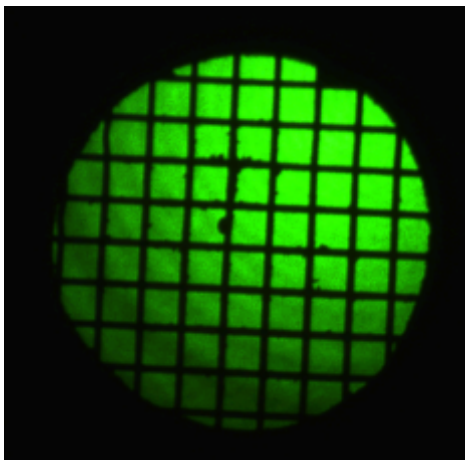


Figure 3: The planar array responsible for the pattern created in Figure 2.

Should the elements be idealised point radiators, the larger Fraunhofer pattern disappears and the higher spatial frequency radiation pattern remains. Note that the parts of the radiation not within the brightest central spot - the sidelobes - are undesirable but inevitable given the physics of diffraction [10].

5.2 Phase Shifter Technologies and Their Fault Scenarios

Phase shifters are a critical component of beamforming, and their specific implementation affects the types of fault an array could be subject to. The literature presents a diverse landscape of phase shifter technologies, which can be broadly categorized by implementation platform (electronic, MEMS, hybrid), control type (analog vs digital), and passivity (passive vs active) [4]. Each category presents distinct advantages, limitations, susceptibilities to faults, and optimisation methods. The scope of this project focuses on electronic phase shifters.

Electronic phase shifters are ubiquitous in modern arrays and are the most common approach [4]. They benefit from monolithic integration and fast switching. The working principles fall into three categories: vector-sum, switched-line, and reflector.

For the vector-sum (sometimes referred to as “vector modulator”) phase shifter, an “in-phase” and “quadrature” (quarter cycle phase offset) signal are combined with variable gains to form arbitrary phases at the output, as shown in Figure 4 [12]. The use of variable gain amplifiers (VGA) makes the vector modulator an active phase shifter, and gives the phase shifter the additional ability to control the amplitude of each radiating element. Since the phase is arbitrary, this is considered an analog phase shifter, which

offers continuous phase control, theoretically enabling infinite resolution. Noise and bias drift introduce errors in the output phase, potentially damaging the radiation pattern, but can be mitigated with calibration.

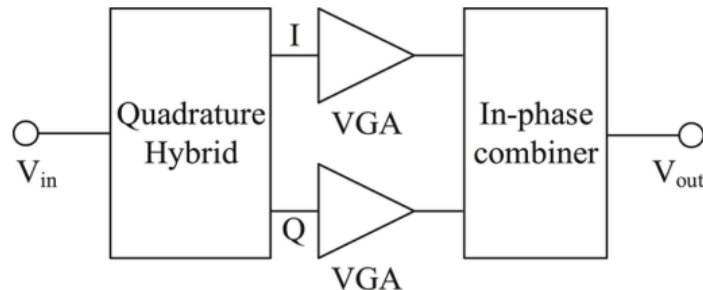


Figure 4: A vector sum phase shifter, generating an I (in-phase) and Q (quadrature) signal with a quadrature hybrid, then applying a variable gain amplifier, and combining the two signals with an in-phase combiner to produce an output signal with arbitrary phase and amplitude [13].

A reflector type phase shifter uses reflectors to introduce phase shifts. One implementation utilises the varactor diode or varicap, where the voltage-dependent capacitance of a reverse-biased P-N junction is taken advantage of to change the RF reflectivity of the component which includes a phase offset [14]. Incoming signals are routed towards the reflector - in this case the varicap - and a controllable phase offset is introduced when the signal reflects off of the reflector depending on the reverse bias voltage. This is a passive, analog phase shifter.

Switched-line phase shifters as shown in Figure 5 utilise feed lines of different lengths connected in junctions that form a choice for the RF signal to travel through [15-17]. Switched-line phase shifters introduce a new paradigm for phase shifting - digital phase shifting. Since the choice of phase delay of each path is pre-set, the main way to cover a large number of possible phase delays is with a series of such switched-line modules for each element, each module implementing an exponentially decreasing portion of the phase space to be delayed (e.g. $\frac{1}{2}$, $\frac{1}{4}$, $\frac{1}{8}$, ...). This results in the control of such phase shifters using binary words, where each bit represents the control signal to one switched-line module. Quantisation error is introduced that slightly deviates from the ideal radiation pattern. Failure of any switch or microstrip line compromises the available set of phases that can be reached.

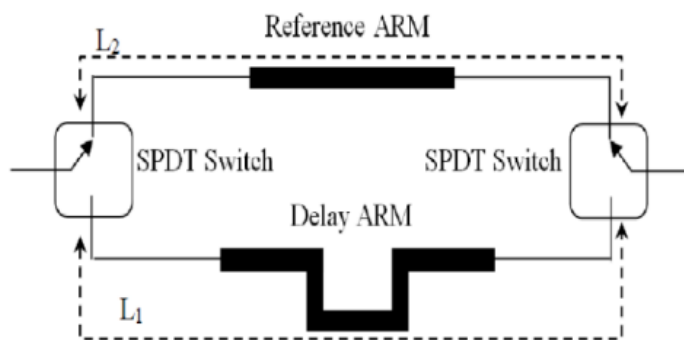


Figure 5: A switched-line phase shifter, with switches that direct the RF signal through a choice of two paths, one representing the no-phase-offset, one representing a phase delay [18].

A distinct implementation incorporating both switched-line and reflector principles is of interest. It uses hybrid couplers shown in Figure 6 - networks that guide a signal away to another path, then return to an original path - to redirect the RF signals towards a fixed reflector gated by PIN diodes. The microstrip path lengths that lead to the reflectors determine the phase delay. The diodes determine whether the signal

travels the extra path to be reflected or not [19-22]. The “I” junction (intrinsic junction) of the PIN diode allows the diode to have a very low capacitance when in reverse bias, emulating an open circuit in the RF domain. These can be made very compact and lightweight, suitable for satellite missions where weight is a strong constraint. However, the fragile diodes used can be damaged and the radiation pattern compromised.

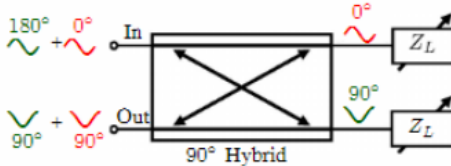


Figure 6: A hybrid coupler. Consider the top path to be the reference. When the input signal splits, the part that travels to the bottom right gains a quarter-cycle phase offset. When the two split signals reflect and propagate towards the top left, they will have a half-cycle phase offset with each other, destructively interfering. The parts that propagate towards the bottom left to the output, will be in-phase again, constructively interfering. The routing of a signal to and from a reflector is achieved [23].

The advantages, limitations and fault scenarios of the electronic phase shifters are summarised in Table 1.

Table 1 - Characteristics of common electronic phase shifter designs derived from their categories and working principles.

Type	Advantages	Disadvantages	Possible Fault Scenarios
Vector-sum (analog, active) [12, 13]	Continuous phase control; high resolution; low insertion loss; amplitude control	Complex circuit; needs accurate I/Q generation; requires calibration; higher power draw	Thermal drift; noise; bias voltage drift
Varactor based (analog, passive) [14]	Continuous phase control; high resolution; compact and low power	Highly nonlinear under large signal levels; sensitive to temperature and bias voltage; narrowband	Varactor breakdown due to over-voltage; thermal drift causing phase instability; noise
Switched-line (digital, passive or active) [15-18]	Simple architecture; capable of broadband handling with design effort	Resolution limited by bit count; bulky if large phase shift ranges are required	Damaged switches; interconnect failure due to thermal stress
PIN diode gated reflector (digital, passive) [19-23]	Fast switching; compact and scalable; low insertion loss	Resolution limited by bit count; requires a bias network	Diodes fail to switch (burned or leakage); diodes lost due to minor impact; interconnect failure due to thermal stress

5.3 Fault Models

Recent work has focused on improving the robustness of phased arrays under failure conditions. These works each assume a fault model.

Several studies considered total or random failure modes - either elements drop out entirely, or the output phases of phase shifters are kicked to different phases due to noise or hardware imperfections [25-27]. The

failure mode of element dropout is the most broadly applicable, where all the phase shifters can become damaged or lost, and the choice to switch off the element is made. The failure mode of random kicks is applicable to analog phase shifters like the vector-sum and varactor-based phase shifters, due to their thermal and bias condition drifts. Tang et al. considered phase deviations introduced by the antenna surface deformations [28]. This falls in the category of the random-kicks.

Munsif and Ullah identified an additional failure mode as deviations of entire phase shifters to random phase states and being locked there, without the phase shifter dropping out [7]. They further identify that the central elements contribute more to the damage of the radiation pattern than edge elements. Zhou et al. considered radiation pattern impairment due to structural degradation, such as radome ablation [29]. This is a damage to the radiation pattern on the pattern level, not the phase level.

The fault models considered by the literature are summarised in Table 2.

Table 2 - Fault models in the context of radiation pattern recovery and robust beamforming, considered by current literature.

Fault model	Description	Available Optimisation
Element drop-out [25-27]	Irreparable damage to the phase shifter or element; decision to switch off an element.	The phases of the remaining elements.
Fixed kicks to each phase shifter output [25-28]	Could be caused by bias condition drift; antenna surface deformation; calibration error. Each phase shifter is still controllable.	The phases of all elements.
Entire phase shifter stuck to random phase [7]	The malfunctioning phase shifter is not controllable, and also remains on.	The phases of the remaining elements.
Direct radiation pattern damage [29]	Could be caused by radome ablation. The deviation happens at the pattern-level.	The phases of all elements.

5.4 Beamforming Algorithm Optimisation Techniques

The same studies from Section 5.3 consider techniques to repair the radiation pattern and improve beamforming capabilities. These techniques are applied on the algorithmic level, rather than the hardware repair level. Due to the nonlinear relationship between the radiation pattern and the element phases, these optimisations are performed globally rather than element-wise. The most common methods are population-based iterative algorithms like the Genetic Algorithm (GA) and Particle Swarm Optimisation (PSO), which are effective in high-dimensional search spaces, but do not guarantee optimality. They both utilise an objective function that can incorporate multiple objectives, such as Peak Beam Power (PBP), Peak SideLobe Level (PSLL), and Mean Squared Error (MSE).

The GA algorithm is shown in Figure 7. Candidates are called chromosomes, each with a fitness according to some objective function. A population of randomised chromosomes is iteratively evaluated, as the higher fitness members reproduce (implemented with gene cross-over) and mutate (implemented with random gene changes). Termination criteria could be convergence, or reaching a threshold in the objective function, or reaching a max iteration. Saleem et al. demonstrated a phase-only GA restoring beamforming for failed

center elements in a 4×2 array [30]. GA easily handles multiple parameters and constraints (e.g. SLL vs main-beam trade-offs), but may require many evaluations for convergence.

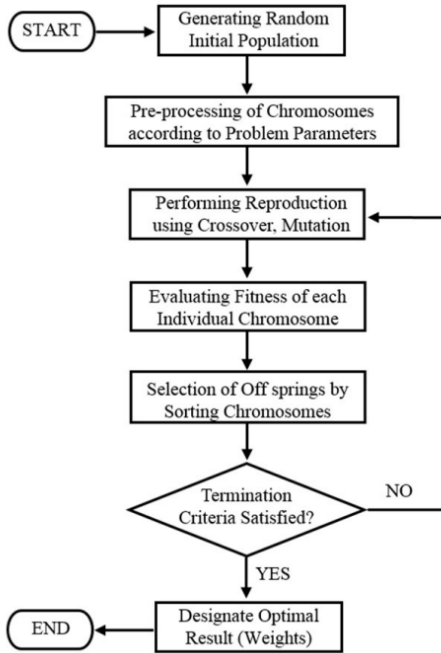


Figure 7: The genetic algorithm [30].

The PSO algorithm is shown in Figure 8. It is inspired by swarm behaviour. Each member of the swarm occupies their own position in the search space, and has a velocity through the search space. Their velocity is an aggregation of three factors: a social factor, where they approach the best position found by the population; a cognitive factor, where they approach the best position found by themselves; an inertial factor, where their velocity has momentum and isn't instantaneously responsive. This results in efficient exploration of the search space.

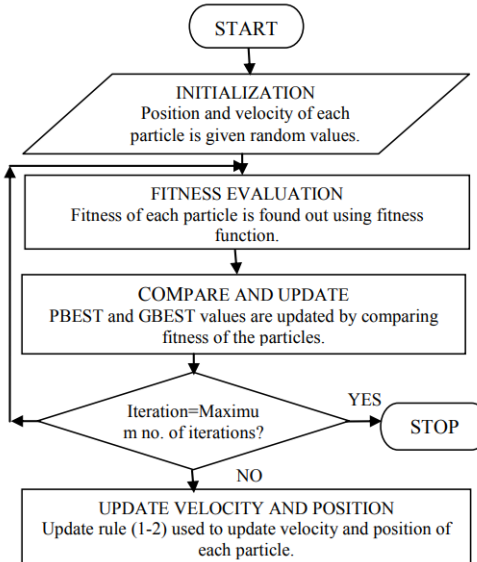


Figure 8: The PSO algorithm [32]. Rule (1-2) calculates the new velocity of each particle according to the social, cognitive and inertial factors, and updates their positions.

Boopalan et al. compared GA, PSO, and pattern-search on a 4×4 array with up to 20% element failures; PSO achieved the best match to the desired pattern, significantly reducing sidelobe errors [31]. Likewise,

Munsif's Multi-Objective-PSO approach used a swarm to balance multiple objectives (gain and sidelobes) in a conformal array [7]. Such algorithms require hyper-parameter tuning, and non-trivial convergence times.

5.5 Research Gap

A clear research gap emerges when considering Table 1 and Section 5.3. The digital phase shifters with fragile components lead to practical scenarios where individual bits in the phase shifter become stuck to either 0 or 1, but still leaving the remaining bits of the same phase shifter operational (e.g. the 2nd bit of a 3-bit phase shifter is stuck at 1, meaning the available phase settings are "010, 011, 110, 111"). This is a novel fault model happening at the bit-level, specific to digital phase shifters, leaving open the option of bit-level optimisation. It can be seen in Table 2 that the literature only considers faults at the pattern level, element level, or phase level.

Moreover, the existing solutions are global optimisations that take time to converge. This often leads to the requirement that all phase settings for all scenarios are pre-computed and stored in memory prior to deployment. Taking advantage of the partially compromised phase shifters, this project proposes a new EElement-wise Optimisation algorithm (ELO) that could achieve near-optimal recovery of the radiation pattern in real-time, allowing for robust beamforming even if new fault states become known during deployment.

6 Methodology and Methods

6.1 Methodology

This project adopted a simulation-driven approach to evaluate and improve the performance of a phased array antenna system under bit-level hardware constraints. This methodology was chosen due to hardware faults in the physical antenna provided, and the prohibitive cost of redesigning a new antenna. Simulation also allows for scaling and parameter sweeps with thousands of trials that are simply unachievable in a physical setting.

The following subsections describe the mathematical model of ideal beamforming and quantised beamforming adopted for this project. These were expanded upon when creating a mathematical model of bit-level faults, and designing the algorithm. The performance of the algorithm was evaluated with Monte-Carlo trials over array parameter sweeps, and compared against baselines of the field.

6.1.1 System Model - Ideal Beamforming

We consider a uniform linear array (ULA) consisting of N isotropic antenna elements arranged along the x -axis with half-wavelength spacing $d = \lambda/2$. Let θ denote the angle of measurement from broadside, and let the desired beam steering direction be θ_0 . The ideal progressive phase shift across elements is given by:

$$\phi_{ideal}^{(n)} = -kdn \sin(\theta_0) = -\pi n \sin(\theta_0), \quad n = 0, 1, \dots, N - 1 \quad (1)$$

where $k = 2\pi/\lambda$ is the wavenumber. The ideal (normalized) array factor can be expressed as:

$$AF(\theta) = \frac{1}{N} \sum_{n=0}^{N-1} w_n e^{jn\pi \sin\theta} \quad (2)$$

where $w_n = e^{j\phi_{ideal}^{(n)}}$ is the complex excitation weight, assumed to be of unit magnitude for all elements.

6.1.2 System Model - Quantised phase shifters

Each element is equipped with an M -bit digital phase shifter, allowing for 2^M discrete phase states uniformly distributed over the interval $[0, 2\pi]$. The ideal phase shift resolution is thus $\Delta\phi = \frac{2\pi}{2^M} = \frac{\pi}{2^{M-1}}$.

Each ideal phase $\phi_{ideal}^{(n)}$ must be quantized to the nearest representable value given the M -bit resolution.

The set of quantized phase values is:

$$Q = \{0, \Delta\phi, 2\Delta\phi, \dots, (2^M - 1)\Delta\phi\}$$

We represent each M -bit phase setting as a binary word $\bar{b} = b_{M-1} \dots b_2 b_1 b_0$ that would reproduce the quantized phase, with b_{M-1} representing the most significant bit (MSB). \bar{b} is calculated with Equation (3).

$$\bar{b} = DecToBin(Round(\phi_{ideal}^{(n)}/\Delta\phi)) \quad (3)$$

The actual quantized phase applied to the n -th element is:

$$\phi_{quantised}^{(n)} = \Delta\phi \sum_{i=0}^{M-1} b_i^{(n)} 2^i \quad (4)$$

6.2 Method

6.2.1 Physical Antenna Array Inspection

A faulty physical antenna was provided by the “Airborne Passive Radiometer for High Resolution Soil Moisture Monitoring” (DP160104233) project, as shown in Figure 9.

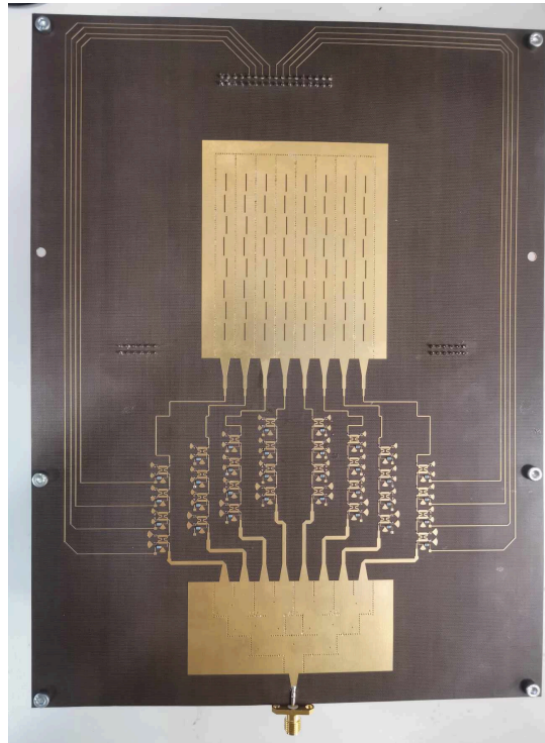


Figure 9: An 8x8 Ku band phased array antenna implemented with Surface Integrated Waveguide (SIW) technology.

The antenna was an 8x8 Ku band planar phased array implemented with Surface Integrated Waveguide (SIW) technology, which has superior performance against microstrip patches due to the patches experiencing dielectric loss [33, 34]. Only one dimension had beam-steering capability, and for the purposes of this analysis, the array behaves like a 1x8 uniform linear array (ULA). The phase shifters were implemented with PIN diodes and hybrid couplers, with a 4-bit resolution, as shown in figure 10.

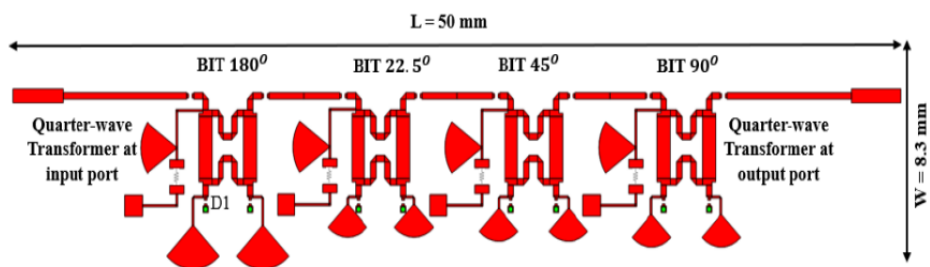


Figure 10: a phase shifter for a single strip of the antenna array. The 4 bits allow for a resolution of 22.5 degrees in each phase.

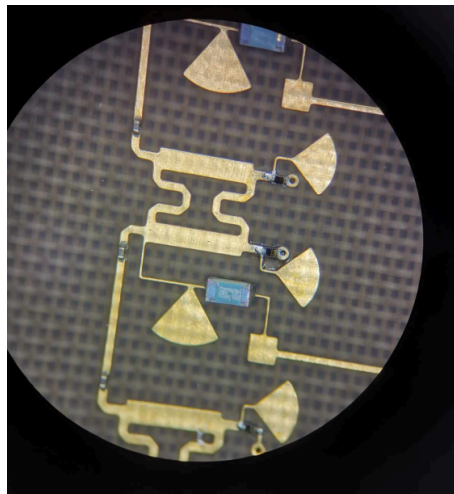


Figure 11: Close up of a single bit of a phase shifter. The two black square-shaped components are the PIN diodes.

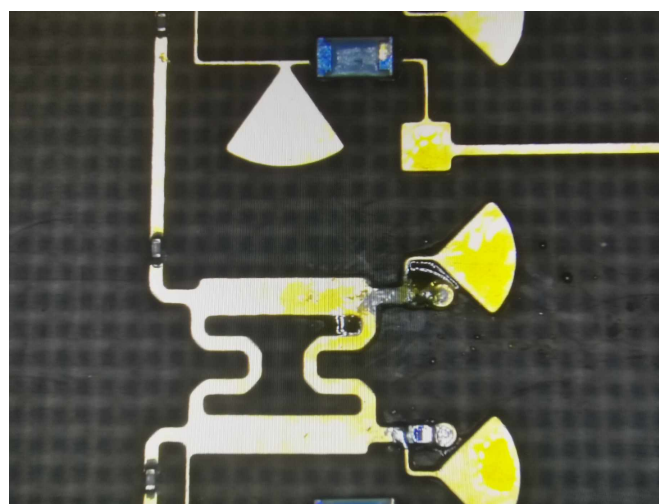


Figure 12: A missing PIN diode due to heat stress.

The array was inspected under a microscope. Figure 11 shows the network that implements a single bit in a phase shifter. Figure 12 shows a missing PIN diode which would result in a bit-level constraint.

6.2.2 Bit-level Fault Model Construction

To simulate realistic hardware limitations in digital phase shifters, a mathematical model was developed for the bit-level faults.

6.2.3 Simulation of Quantisation and Bit-level Faults

Using Python, a custom simulation environment was built to model ideal, quantised and faulty phase outputs across the array. Two sub categories of faults were considered:

1. **MSB Failures:** The most significant bit of certain elements (i.e., b_{M-1}) are stuck at either 0 or 1 due to diode damage or loss. This makes an entire half-cycle of potential phase shifts inaccessible to the phase shifter. This failure mode becomes likely for low-resolution phase shifters (e.g., $M = 4$).
2. **Random Bit Failures:** A more general fault model in which any subset of bits (not necessarily contiguous or most significant) may be stuck, and the failure pattern is randomly assigned across the array.

The main feature of the simulation is the visualisation of the antenna array factor according to Equation (2).

6.2.4 Designing Element-wise Local Optimisation (ELO) algorithm

To mitigate the radiation pattern degradation caused by faulty phase shifters, a novel Element-wise Local Optimisation (ELO) algorithm was developed. Rather than globally searching the solution space iteratively, ELO optimised the phase setting of each individual bit while holding the faulty ones constant.

6.2.5 Implementing GA and BPSO

For comparative purposes, two population-based global optimisation algorithms - Genetic Algorithm (GA) and Binary Particle Swarm Optimisation (BPSO) - were implemented.

These algorithms were adapted to handle the constrained phase state space introduced by bit-level faults. BPSO is an adaptation of PSO for a multi-dimensional binary search space, where the velocity is replaced by probability of swapping a bit. Each candidate solution encoded the discrete phase settings of all array elements, respecting individual fault constraints i.e. binary vectors of length $2^M - n_{stuck\ bits}$. The gene crossover of GA was implemented instead as direct (not necessarily contiguous) bit exchanges.

The fitness function for both algorithms was defined as the negative of the normalised MSE between the candidate's radiation pattern and the ideal one, as shown in Equation (5):

$$MSE_{norm}(AF) = \frac{1}{\sum_i |AF_{ideal}(\theta_i)|^2} \sum_i |AF_{ideal}(\theta_i) - AF(\theta_i)|^2 \quad (5)$$

Standard parameters were used for GA (crossover rate, mutation probability, population size) and BPSO (inertia weight, cognitive and social coefficients), with tuning performed experimentally for best performance according to the MSE_{norm} .

6.2.6 Monte Carlo Simulations of the Optimisation Algorithms

To statistically evaluate robustness and generalisability, Monte Carlo simulations were conducted for each optimisation algorithm, across all levels of faults (proportion of total bits stuck).

For each trial, a random fault pattern was generated by disabling bits in a subset of the phase shifters. The optimisation algorithms were then applied to recover a near-ideal beam pattern. This process was repeated for 1000 trials per algorithm, per number of stuck bits. Multi-core processing was utilised to reduce the total time of simulation.

Key performance metrics - including MSE_{norm} , PBP, PSLL, and convergence speed - were recorded. This enabled a rigorous comparison across a range of fault distributions and fault severities, with criteria commonly found in literature. Equations (6) and (7) define PBP and PSLL respectively.

$$PBP(AF) = 20 \log_{10} |AF(\theta_0)| \quad (6)$$

$$PSLL(AF) = \frac{20 \log_{10} \max(AF(\theta))}{PBP(AF)}, \theta \notin [\theta_0 - \frac{\text{beamwidth}}{2}, \theta_0 + \frac{\text{beamwidth}}{2}] \quad (7)$$

For the purposes of this evaluation, the beamwidth is defined as the angular span of the main beam between the first nulls on either side. For a 1x8 ULA, the beamwidth is approximately 28.65° .

7 Results and Discussion

7.1 A Mathematical Model for Bit-level Faults

The mathematical model was developed assuming for each phase $\phi^{(n)}$ an ideal desired phase is known, which is then quantised by the set Q, and converted into a binary word according to Equation (3).

In general, for each phase shifter element n, denote a set of bit positions $P_0^{(n)}$ with values stuck at 0, and a set of bit positions $P_1^{(n)}$ with values stuck at 1. This overrides the element phase to:

$$\phi_{faulty}^{(n)} = \Delta\phi \cdot \left(\sum_{i=0, i \notin P_0^{(n)} \cup P_1^{(n)}}^{M-1} b_i^{(n)} 2^i + \sum_{i \in P_1^{(n)}} 2^i \right) \quad (8)$$

which distorts the array factor according to Equation (2).

7.2 Simulation of Quantisation and Bit-level Faults

A simulation was created in Python, setting $N = 8$ and $M = 4$. The beam steering was occurring along the x -axis. The steering angle θ was measured counterclockwise about the y -axis. The normalised array factor was calculated for an 8x8 planar array.

Figure 13 shows the array factor of ideal and quantised phases superimposed on each other. It can be seen that even a low-resolution quantisation of 4-bits displays exceptional accuracy to the ideal array factor.

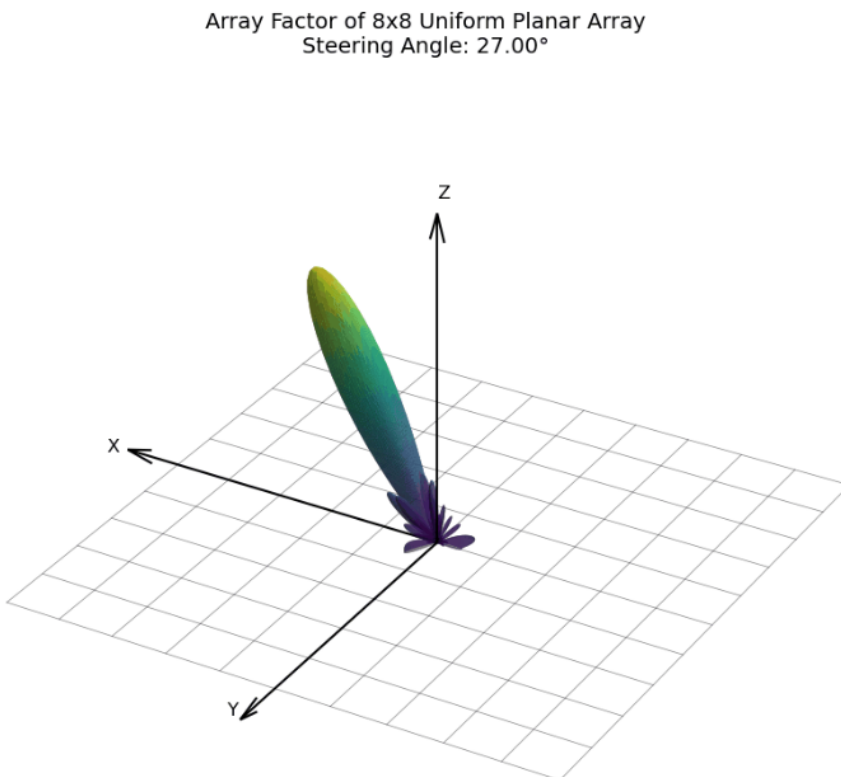


Figure 13: Ideal array factor and quantised array factor for an 8x8 planar array. The quantised array factor is not visible due to matching almost exactly with the ideal array factor.

The random failure mode and MSB failure mode were simulated using the model in Equation (8), shown in Figure 14 and figure 15 respectively.

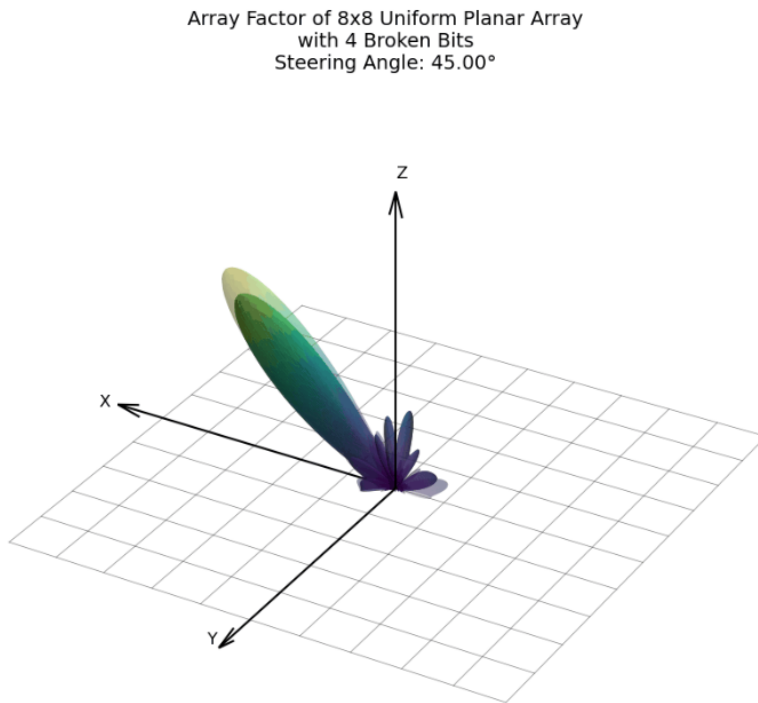


Figure 14: A typical radiation pattern for a random bit failure (solid colors). The translucent pattern shows the ideal array factor.

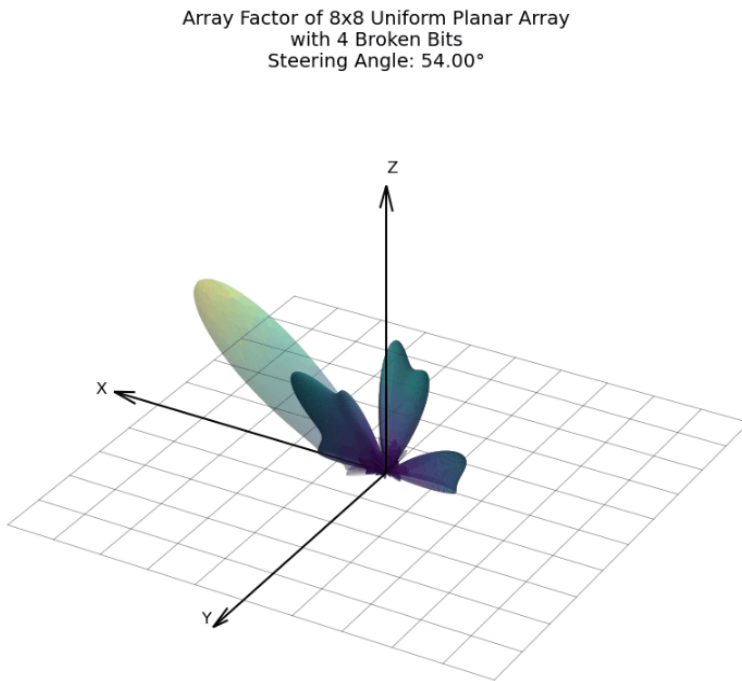


Figure 15: A typical radiation pattern for a MSB failure (solid colors). The translucent pattern shows the ideal array factor.

The MSB failures resulted in a significantly more damaged radiation pattern compared to the random failure of the same broken bit count. The patterns typically have PSLLs of greater than 0dB, meaning the main beam is overpowered by the side lobes and the array is useless for any sensing applications.

Animations were created to further illustrate the effect on the radiation pattern at different steering angles. The deviated pattern was found to be drastically different for the same bit-level fault states, across the steering angles.

Quantitative and statistical analysis of the impact will be illustrated in the Monte Carlo simulations in Section 7.5.

7.3 The ELO Algorithm and its Performance

We assume that phase settings had been optimized for the array prior to the bit-level faults, using any of the optimization algorithms in existing literature, and stored in a codebook i.e. $\phi_{desired}^{(n)}$ is known. For this project, $\phi_{desired}^{(n)} = \phi_{ideal}^{(n)}$ according to Equation (1).

The goal of the proposed self-repair algorithm is to minimize the distortion in the radiation pattern away from this optimized pattern without the need to recompute the codebook. The fault state $\{P_0^{(n)}, P_1^{(n)}\}$ is assumed to be known via hardware inspection prior to deployment or any fault-monitoring system during deployment.

The ELO algorithm is shown in Figure 16. Given the fault state, each element n has a constrained set of achievable phase values $Q_{avail}^{(n)} \subseteq Q$ and a set of binary words $B_{avail}^{(n)}$ that produce those phase values. Given the existing optimization codebook during operation, each element has a desired quantized phase value $\phi_{desired}^{(n)}$ produced by the binary word $\bar{b}_{desired}^{(n)}$. Suppose $\phi_{desired}^{(n)} \notin Q_{avail}^{(n)}$. In the ELO algorithm, the reachable phase ϕ^* with the minimum angular distance modulo 2π to the desired phase is chosen, to replace the desired phase. This corresponds to the $\bar{b}^* \in B_{avail}^{(n)}$ with the minimum distance modulo 2^M to $\bar{b}_{desired}^{(n)}$ desired.

Algorithm 1 Element-wise Phase Setting Repair

Input: Desired beamforming vector $w \in C^N$, phase shifter resolution M , sets of bit positions stuck at 0 for each element $\{\mathcal{P}_0^{(1)}, \mathcal{P}_0^{(2)} \dots \mathcal{P}_0^{(N)}\}$, sets of bit positions stuck at 1 for each element $\{\mathcal{P}_1^{(1)}, \mathcal{P}_1^{(2)} \dots \mathcal{P}_1^{(N)}\}$

Output: Repaired beamforming vector $w^* \in C^N$

```

 $w^* \leftarrow w$ 
 $\Delta\phi \leftarrow 2\pi/2^M$ 
for  $n = 1$  to  $N$  do
     $\phi_{desired} \leftarrow \angle w_n$ 
     $b_{desired} \leftarrow \text{DecToBin}(\text{Round}(\phi_{desired}/\Delta\phi))$ 
     $B \leftarrow \text{AvailableBinaryWordSet}(M, \mathcal{P}_0^{(n)}, \mathcal{P}_1^{(n)})$ 
    if  $b_{desired} \notin B$  then
         $b^* \leftarrow \arg \min_{b \in B} \text{WrappedDistance}(b, b_{desired})$ 
         $\phi^* \leftarrow \Delta\phi \times \text{BinToDec}(b^*)$ 
         $w_n^* \leftarrow e^{j\phi^*}$ 
    end if
end for
return  $w^*$ 

```

Figure 16: The ELO algorithm.

Simulations were run to visualise the effect of the ELO algorithm on various fault states. For visual clarity, only a slice of the pattern through the xz -plane was included. This is shown in Figure 17.

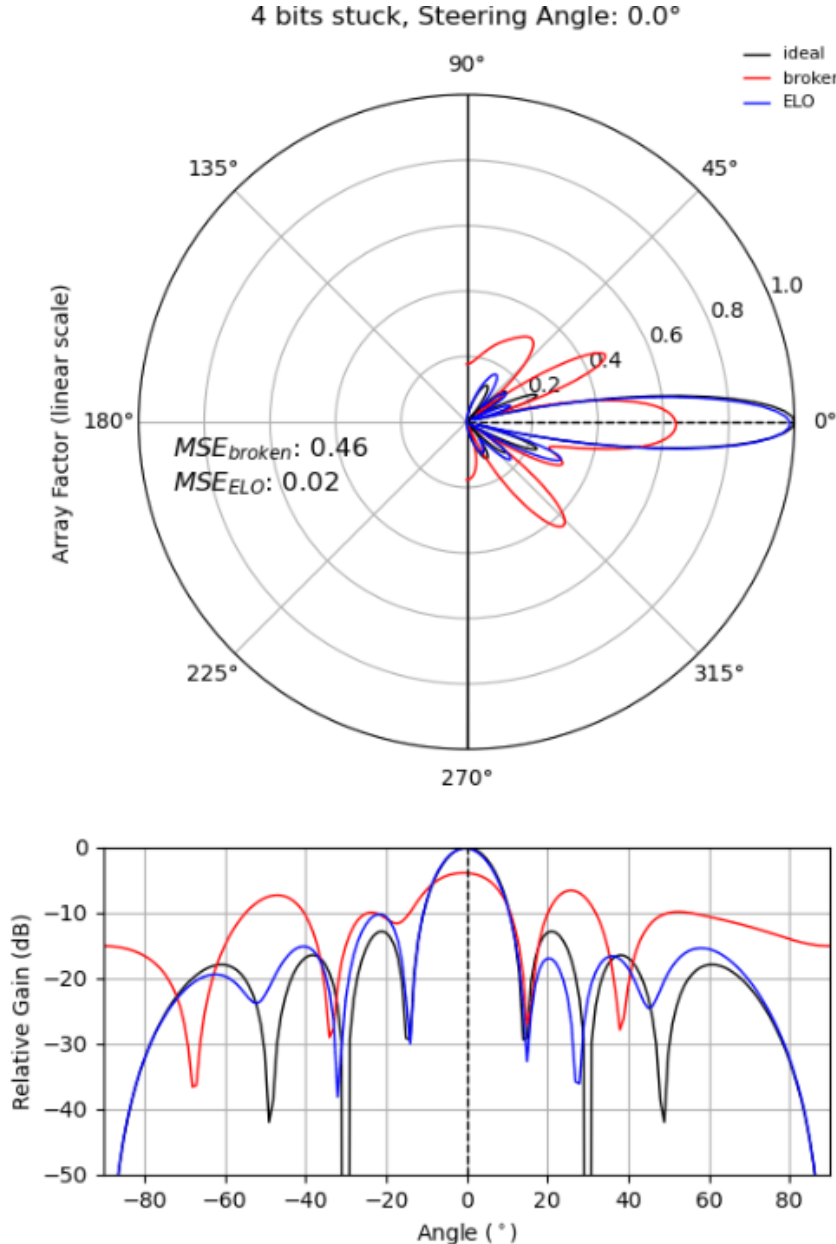


Figure 17: A typical radiation recovery by the ELO algorithm..

The ELO algorithm was able to achieve a near-optimal radiation pattern even for severely distorted patterns. There was no noticeable difference between the MSB and random failure modes. The fact that MSB failures do not drastically decrease the effectiveness of the ELO algorithm could be understood with the following example:

- $\bar{b}_{desired}^{(n)} = 0000$
- $P_0^{(n)} = \{\}, P_1^{(n)} = \{3\}$
- $\bar{b}_{faulty}^{(n)} = 1000$

- $\bar{b}_{faulty}^* = 1111$

Which results in a wrapped phase deviation of only 22.5° . The original phase deviation of 180° has been reduced eight-fold. In general, in the worst-case scenario, the ELO algorithm reduces the phase deviation by a factor of 2.

The statistical behaviour of ELO will be elaborated in the Monte Carlo simulations in Section 7.5.

7.4 The Performance of GA and BPSO

The GA and BPSO algorithms were tuned until no noticeable improvement could be made. The resulting hyper-parameters are summarised in Table 3 and Table 4 respectively.

Table 3 - Hyper-parameters of GA.

Parameter	Value
Population Size	50
Mutation Rate	0.1
Crossover Rate	0.7
Selection Filter	Top 10%
Stop after Stagnation of:	12 generations

Table 4 - Hyper-parameters of BPSO.

Parameter	Value
Population Size	60
Cognitive Coefficient	1.7
Social Coefficient	2.0
Inertia	0.35
Stop after Stagnation of:	15 generations

Simulations were run to visualise the effect of the GA and BPSO algorithms on various fault states. This is shown in Figure 18 and Figure 19 respectively.

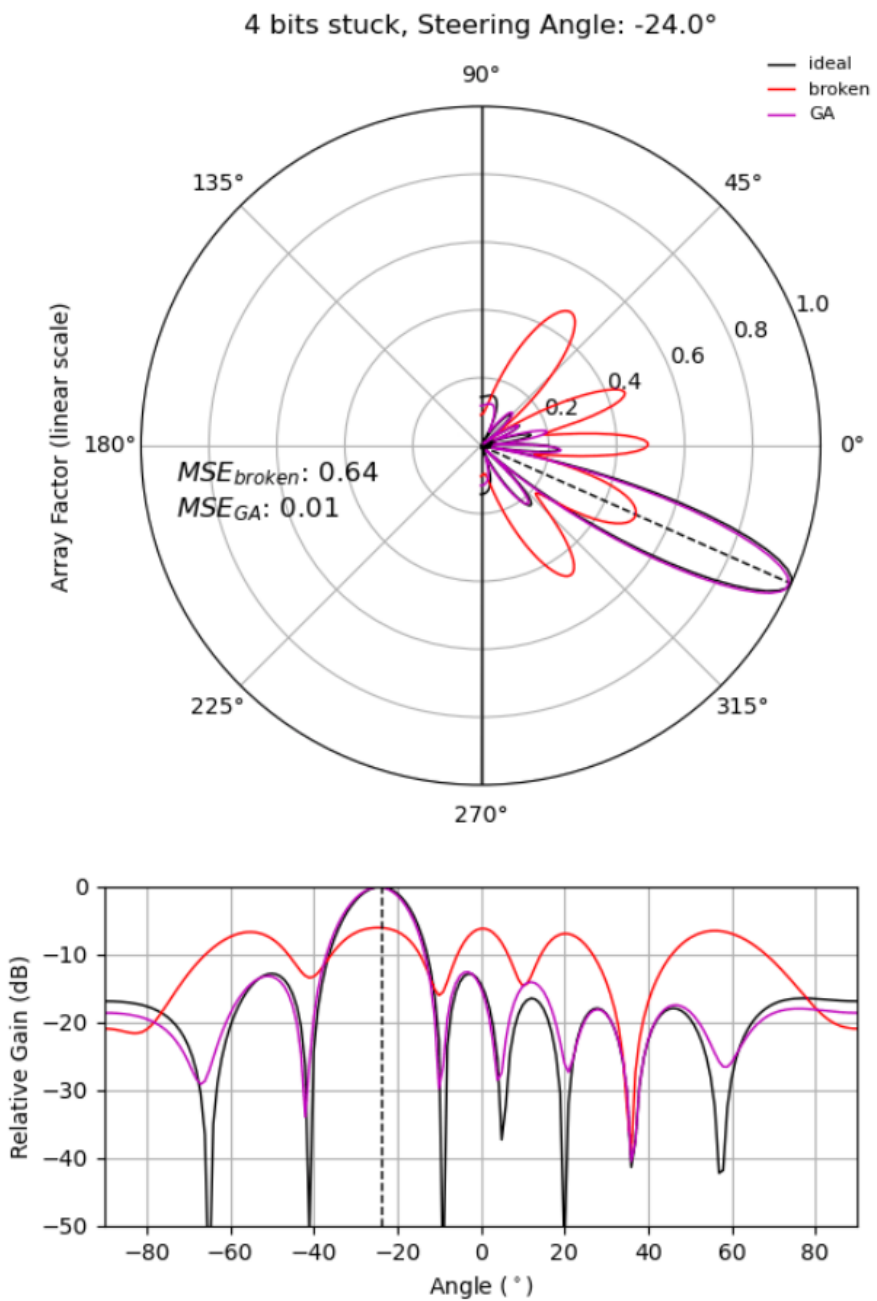


Figure 18: A typical radiation recovery by the GA algorithm.

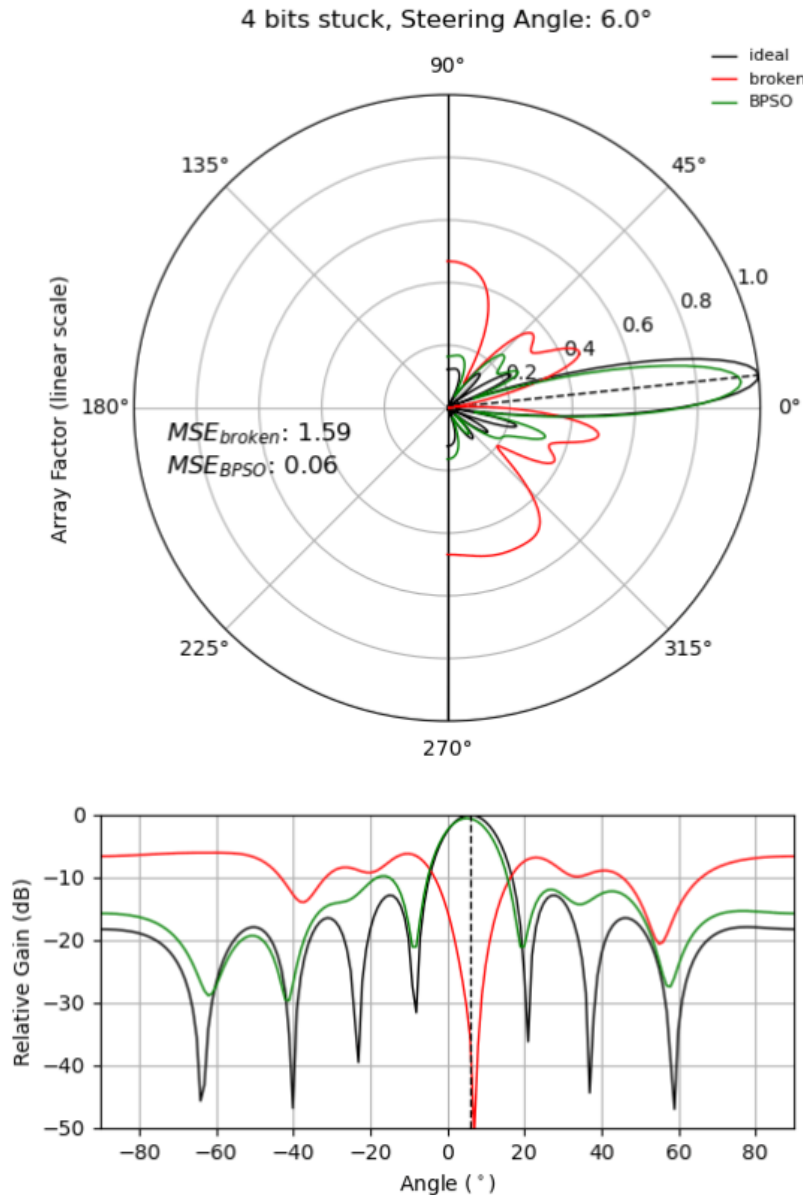


Figure 19: A typical radiation recovery by the BPSO algorithm.

While both GA and BPSO were able to recover the radiation pattern by a lot, reducing MSE_{norm} to below 0.1, the algorithms took a noticeably long time compared to ELO. Convergence took approximately 4 seconds for the GA and BPSO algorithms while ELO took approximately 0.2 ms.

Contrary to literature, the BPSO algorithm was found to converge slower than GA. This was possibly due to the higher stagnation limit that was tuned to optimise the BPSO performance. However, the BPSO generally underperforms GA. This fact will be clearer in the Monte Carlo simulations in Section 7.5.

A comparison of all three optimisation techniques for the same fault state is shown in figure 20. It displays a pattern generally observed across low fault states, where ELO and GA have superior and near optimal performance compared to BPSO. However, the trend does not hold for all fault states, as will be illustrated in Section 7.5.

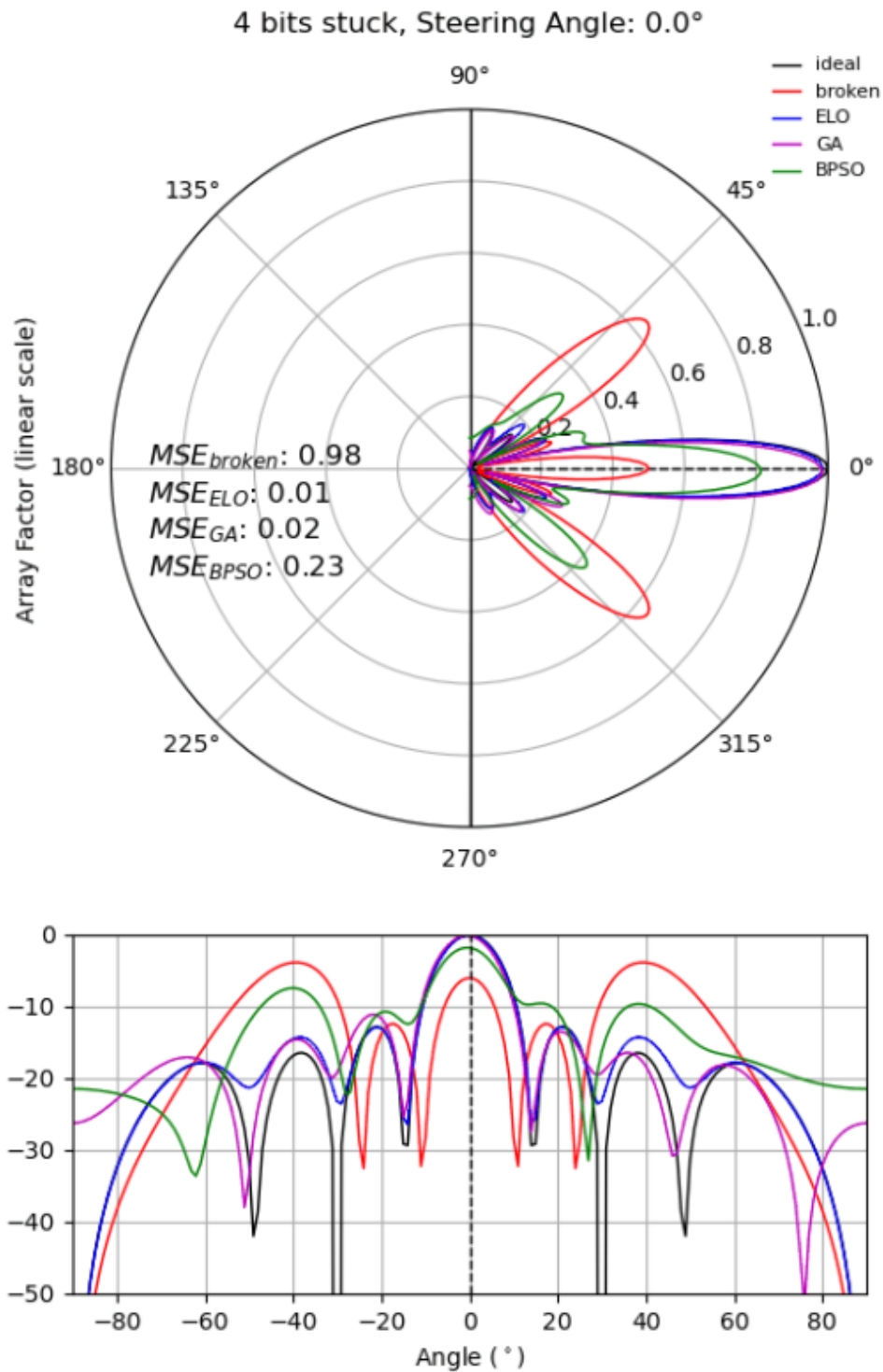


Figure 20: Overlay of the ELO, GA, and BPSO algorithm applied to the same fault state.

7.5 Monte Carlo Simulations

The results of the Monte Carlo simulation were evaluated by metrics defined in Equation (5), (6), (7). These were averaged and plotted against the proportion of failed bits, as shown in Figure 21. 1000 trials were run for each number of stuck bits, for all algorithms.

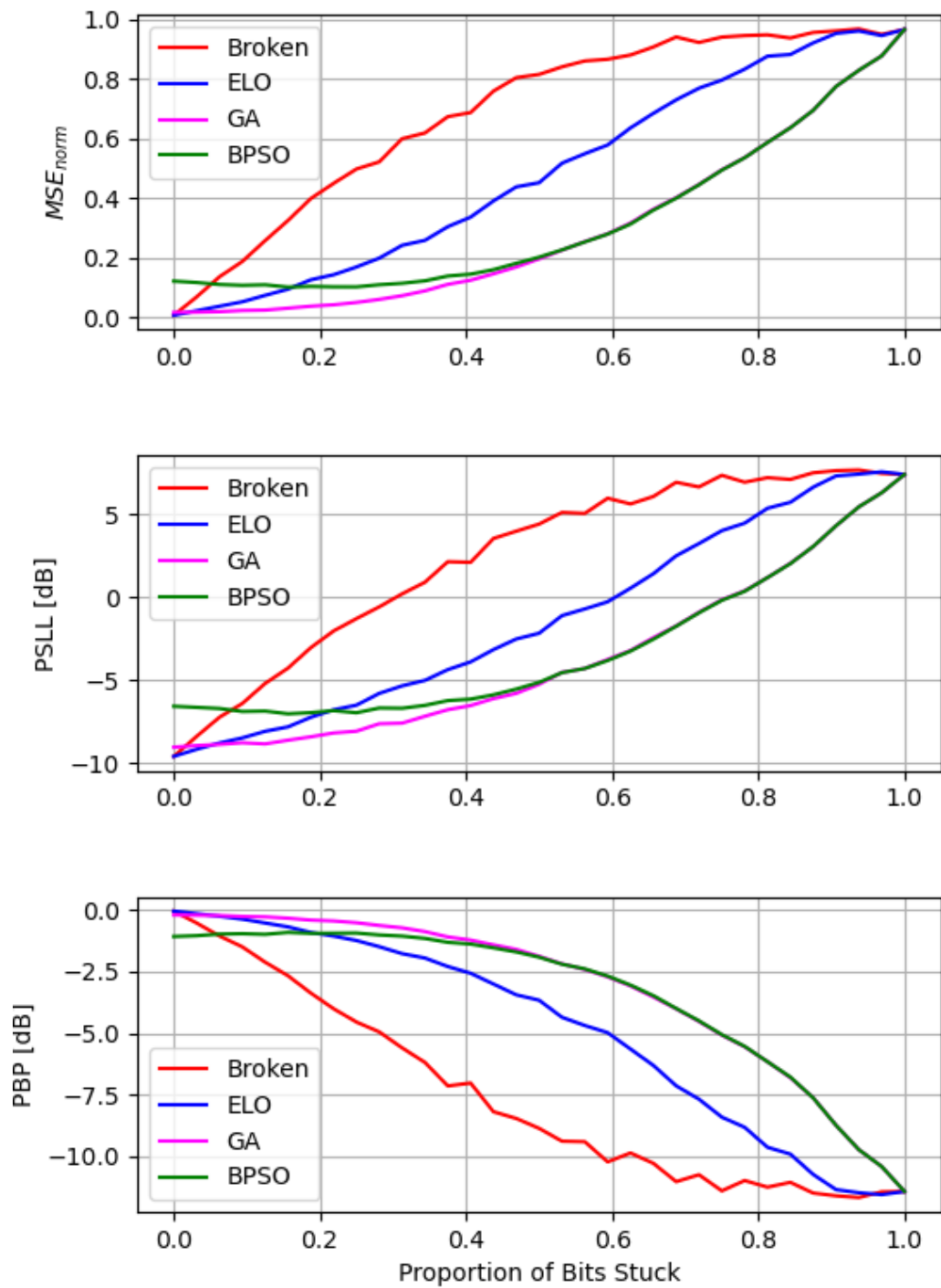


Figure 21: The performance of ELO, GA, and BPSO against the proportions of bits stuck.

All algorithms were able to recover the radiation pattern significantly until a very high proportion of stuck bits. The simulation domain can be split into 3 segments:

1. Proportion of bits stuck ≤ 0.2 . This represents low fault states and is what the literature commonly considers. It is the region of most interest for practical purposes.

2. $0.2 < \text{proportion of bits stuck} \leq 0.6$. This is the region between two major crossover points in the simulation.
3. $0.6 < \text{proportion of bits stuck}$. This region represents a high enough fault rate such that no algorithm can recover the radiation pattern to an acceptable level.

Within Segment 1, GA performed the best with less than -8dB PSLL, near optimal relative peak beam power and mean squared error. ELO came second, with a maximum of -7dB PSLL and near optimal PBP and MSE. BPSO performed the worst with the highest PSLL and MSE, and lowest relative PBP. Segment 1 ends with a crossover point of performance, where BPSO takes over ELO in all metrics.

Within Segment 2, GA still resulted in the best performance, with BPSO converging towards it. ELO's performance rapidly decreased until the PSLL reached 0dB when the proportion of stuck bits reached 0dB, signifying an unusable radiation pattern. Segment 2 ends with the BPSO achieving the same performance as GA.

Within Segment 3, GA and BPSO out performs ELO by approximately 4dB in both PSLL and PBP metrics. However, this region is unlikely to be relevant in practice.

In summary, GA performed the best according to the evaluation metrics for all ranges of fault states. ELO's performance was near optimal for Segment 1 but decreased drastically in Segments 2 and 3, and was overtaken by BPSO. BPSO was the worst performing in Segment 1 but converged to GA by the end of Segment 2. It is interesting to note how GA and BPSO would converge to the same solutions in Segment 3.

A similar simulation was conducted in the MSB fault mode, whose results are shown in Figure 22. Note that the highest end in the domain represents 8 stuck bits i.e. proportion of stuck bits = 0.25.

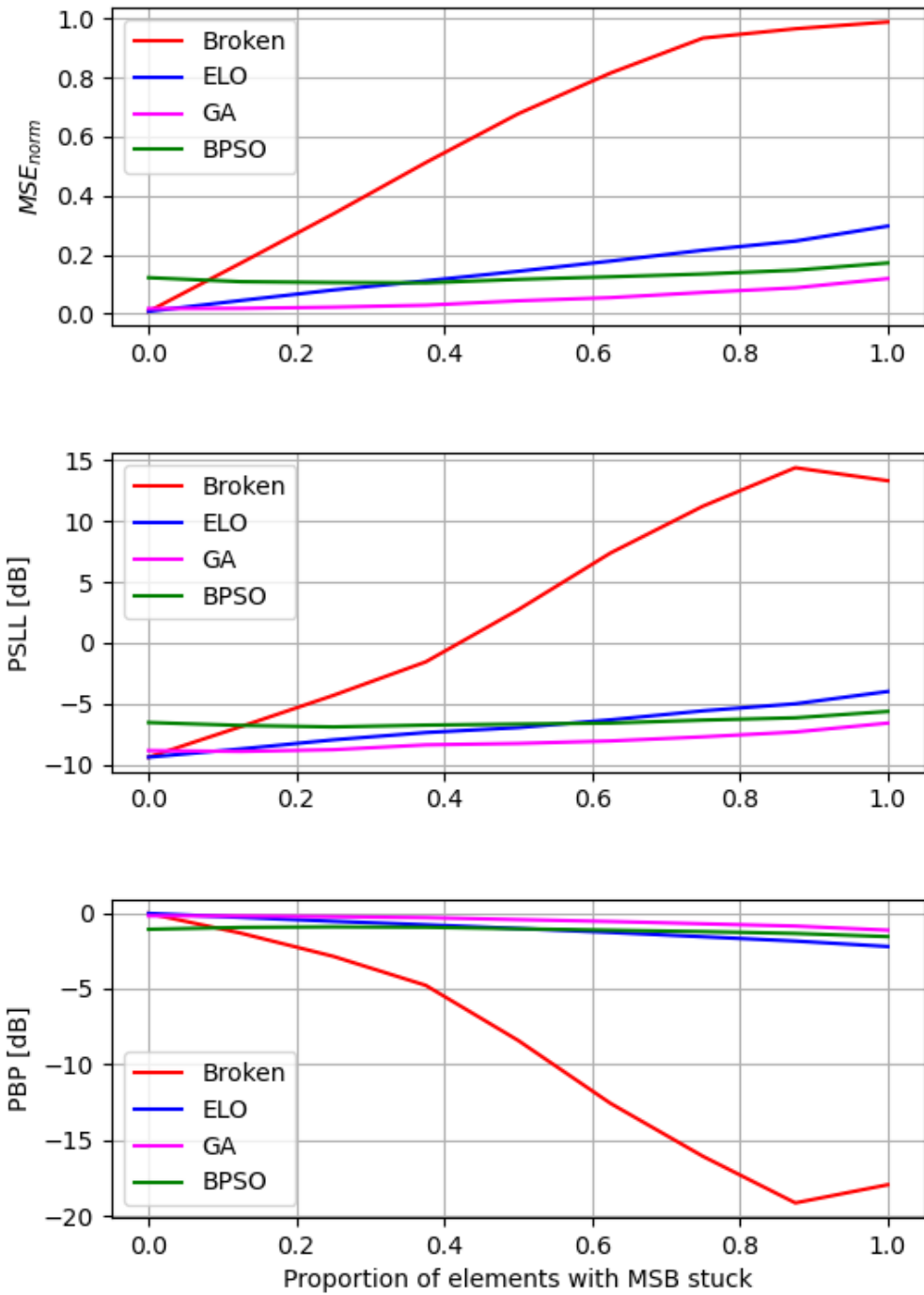


Figure 22: The performance of ELO, GA, and BPSO against the proportions of MSB bits stuck.

Here the effect of MSB failures is demonstrated. Comparing the red traces with the left-most quarter of Figure 21, the MSB failure mode reached near maximum average deviation in the radiation pattern – an MSE of nearly 1, and a PSLL of over 10. Yet, despite the strong deviation in the un-optimised pattern, all three algorithms were able to restore the radiation pattern considerably, reaching a PSLL of roughly -5dB and PBP of -2dB even in the worst case.

The optimisation time for each algorithm was averaged over all the trials, and presented in Table 5. ELO had an average time of 0.2052 ms, while the baselines of the field are over 4 s.

Table 5 - Average run times of the algorithms.

Algorithm	Average Runtime (ms)
ELO	0.2052
GA	4171.7777
Social Coefficient	4601.8420

7.6 Summary of Findings

Bit-level faults were found to severely damage the radiation pattern even for a low number of faulty bits. MSB failure mode had more severe damages compared to the random failure mode.

The proposed ELO algorithm was able to quickly recover most of the radiation pattern within the region of low number of faulty bits that is considered practical. This performance closely matches with the baselines in the field such as GA, and even outperforms BPSO. The low runtime allows the ELO to run in real time, should fault-monitoring systems detect bit-level faults during deployment.

With these results, the aim of developing a fault-tolerant smart beamforming approach to address bit-level faults in the phase shifters was achieved, and validated with simulation.

7.7 Limitations and Future Work

Despite the success of the proposed ELO algorithm in simulation, several limitations remained due to constraints in data acquisition, physical validation, and available failure data.

7.7.1 Simulation-Based Evaluation and Lack of Hardware Demonstration

The primary limitation of this project was the absence of a functioning physical phased array antenna to experimentally validate the fault recovery method. All findings were obtained through simulations. They were highly configurable and controlled but may not fully capture the physical non-idealities and noise present in a real-world deployment. In particular, practical constraints such as thermal effects, mutual coupling, manufacturing tolerances, and dynamic reconfiguration delays could impact the effectiveness of the ELO algorithm when applied to actual hardware. However, this aided in the isolation of variables to the bit-level faults. This gap prevents a full assessment of the algorithm's robustness in deployment conditions.

The lack of physical validation slightly weakens the generalisability of the results. However, since the simulation environment was designed to reflect realistic beamforming constraints, the core conclusions regarding the algorithm's performance remain strong.

7.7.2 Fixed Monte Carlo Sampling Budget

Another limitation was the use of a fixed number of Monte Carlo trials of 1000 per fault count per algorithm. While this provided sufficient statistical stability for comparing algorithm performance trends, it still imposed sampling variance - particularly in regions where the fault distribution was combinatorially large (e.g., around half of faulty bits). Additionally, computational limitations prevented the parameter sweep in the number of antenna elements, and bits per phase shifter.

This limitation may have introduced small fluctuations in the reported average error metrics. However, the consistency of trends across algorithms helps offset this effect.

Using variance-reduction techniques or adaptive sampling could help refine estimates while keeping runtime manageable. Alternatively, performing higher-budget simulations on a cluster or GPU-based system would allow for more exhaustive fault space exploration.

7.7.3 Absence of Statistical Failure Data for Phase Shifter Bits

The study assumed uniform-random stuck-bit distributions due to a lack of empirical failure rate data for PIN diode-based phase shifters. In practice, some bits may be more prone to failure due to thermal stress or layout-specific vulnerabilities. The recovery algorithm was tested against a generic fault case, which may not align perfectly with real-world failure distributions.

This assumption does not invalidate the results but merely leads to a lack of expectation for real world fault levels. Since the study was conducted over all fault states, this was not a significant problem. Collaborating with hardware manufacturers or conducting accelerated aging experiments could provide more realistic failure models, enabling the development of more targeted recovery strategies.

7.7.4 Future Work

Building upon the promising results of this project, several directions could enhance its practical relevance and extend its contribution.

A follow-up project could focus on embedding the ELO algorithm into a real-time fault-monitoring and beamforming system using FPGAs or microcontrollers interfaced with a phased array testbed.

A significant but important extension would be to study how to detect bit-level faults or even predict them during deployment, such that the inputs to the ELO algorithm could be updated automatically in real time. Machine learning methods could be incorporated for such a study. Integrating predictive diagnostics using temperature sensors or usage statistics to anticipate failures before they occur could improve system resilience even further.

8 Conclusion

This project set out to investigate how bit-level faults in digital phase shifters affect the performance of phased array antennas, and to design an algorithmic solution capable of mitigating their impact in real time.

Through the development and validation of the Element-wise Local Optimisation (ELO) algorithm, the project has successfully demonstrated that targeted, lightweight optimisation can recover beamforming performance to near-ideal levels, in the presence of practical, non-catastrophic hardware faults.

Crucially, this work addresses a clear research gap identified in Section 5.3 - namely, that existing approaches in the literature treat faults at the phase, element, or pattern level, but largely ignore the finer-grained bit-level failure modes unique to digital phase shifters. These faults are not merely theoretical; they reflect real-world vulnerabilities in practical low-resolution hardware, where certain bits may fail while leaving others functional. By explicitly modeling this behaviour in Equation (8) and exploiting the remaining bit-level degrees of freedom, the ELO algorithm demonstrates a new simple strategy for fault-aware beamforming.

All core objectives of the project were met:

- bit-level faults were successfully modeled
- a tailored optimisation framework was designed and implemented
- the algorithm's performance was validated through simulation against known baselines such as GA and BPSO.

The results show that ELO competes with and in some cases outperforms traditional global optimisations - while also achieving runtimes suitable for dynamic, in-field adaptation to newly discovered faults. The simplest solution proved to be the most efficient, within the range of fault states of practical concern.

This contribution provides both theoretical and practical value. It enhances the understanding of fault behaviour in digital phase shifters and offers a deployable strategy to improve system resilience without modifying hardware. While further physical validation is needed, this project provides a concrete step toward smarter, fault-tolerant beamforming systems, and opens several avenues for future exploration in real-time diagnostics and adaptive antenna design.

9 Reflection on Project Management

9.1 Project Scope

This project focused on the development of a fault-tolerant beamforming algorithm for phased array antennas using low-resolution digital phase shifters. Specifically, it addressed the impact of bit-level hardware faults—where individual control bits may become permanently stuck-on the antenna's radiation pattern. The scope included modelling such faults mathematically and in simulation, designing an optimisation algorithm (ELO) capable of compensating for them in real time, and evaluating its performance against established techniques such as Genetic Algorithms (GA) and Binary Particle Swarm Optimisation (BPSO). The project was limited to simulation-based validation and did not include hardware implementation or empirical failure data collection, although practical implications and future deployment considerations were discussed.

9.2 Project Plan & Timeline

The project advanced in the following phases. A Gantt chart summary of this is shown in Figure 23.

9.2.1 Phase 1: Literature Review and Experimental Fault diagnosis - 9 weeks

A Ku-band phased array antenna that was designed by a PhD student arrived in week 6 of FYP A. This provided a valuable opportunity to practice the experimental techniques of antenna testing. The antenna had many problems that were fixed during its assembly. A preliminary beamforming algorithm was devised.

9.2.2 Phase 2: Measurement of the Radiation Characteristics - 4 weeks

The return loss at various steering angles, and the radiation pattern at various steering angles, were attempted to be measured for the Ku-band antenna. These results indicated the antenna did not work.

9.2.3 Phase 3: Repairing the Antenna- 7 weeks

The antenna was studied in detail and many faults were observed and mitigated. However, the control board for the phase shifters did not function correctly. None of the BJT networks were outputting the correct voltage.

9.2.4 Phase 4: Pivot and Novel Fault Model Identification - 5 weeks

With the supervisor's guidance, we pivoted the project to study fault-tolerant beamforming on the algorithmic level. One specific fault model - the bit-level faults associated with the PIN diode losses and damages - were deemed interesting to study.

9.2.5 Phase 5: Simulation and Data Collection - 3 weeks

The fault was modelled and simulated in python. A preliminary simple algorithm was devised to mitigate this fault. The algorithm was discovered to work better than expected. Various statistical trials were conducted.

9.2.6 Phase 6: Analysis and Comparison against baselines - 3 weeks

A final literature review was conducted to ensure we didn't misidentify a gap during our first literature review. GA and BPSO algorithms were implemented to compare against the ELO we wrote.

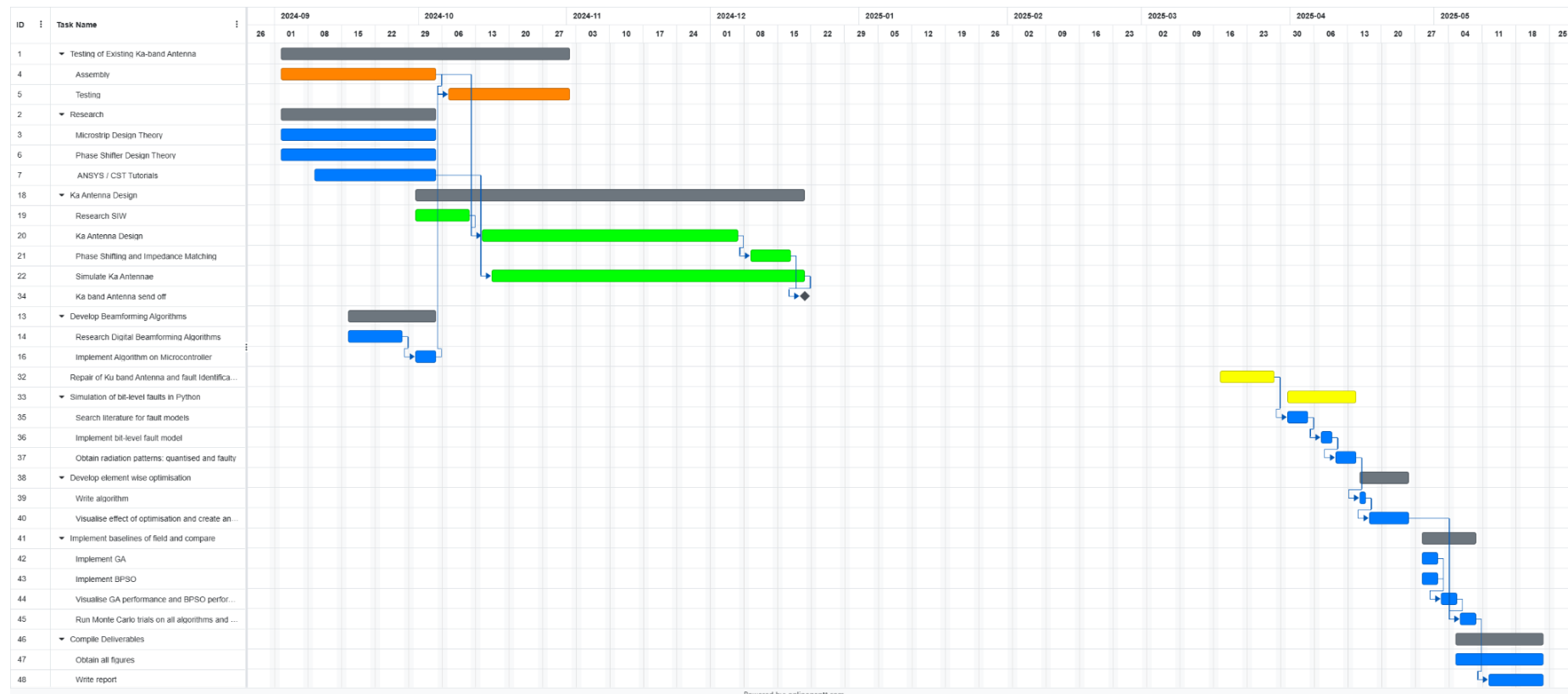


Figure 23: updated Gantt chart for this project.

9.3 Reflection on Project

This project evolved significantly from its original plan, and the pivot in direction ultimately led to a more focused and impactful outcome. Initially, the goal was to design and characterise a physical phased array antenna in the lab. However, after encountering a faulty antenna module early in the process, the timeline was delayed, and the original hardware-dependent plan became increasingly impractical. Based on feedback from the progress report and discussions with my supervisor, I made a strategic decision to narrow the scope to algorithmic development and simulation. This shift enabled me to pursue a deeper exploration of the problem space, ultimately leading to the development of the ELO algorithm and the study of a novel fault model.

Although the timeline slipped during the hardware troubleshooting phase, the pivot allowed me to regain momentum. All tasks and sub-tasks related to the revised scope were completed, including fault modeling, algorithm design, benchmarking, and performance evaluation. The major success of the project lies in demonstrating that beamforming performance can be recovered in real time under bit-level fault conditions - a gap in the current literature that this project addressed. The result that the simplest algorithm was the most efficient was a pleasant surprise amidst the challenges outside of my control.

Reflecting on my individual performance, I am satisfied with how I handled unexpected challenges. The shift away from physical hardware required flexibility, quick decision-making, and effective time management. I also deepened my understanding of algorithmic problem-solving and optimisation under hardware constraints. However, one area for improvement is contingency planning. Earlier identification of hardware risks and a parallel simulation track could have mitigated the initial timeline delays. In future projects, I would implement more rigorous risk assessment early on and define clear fallback options.

This project also taught me the value of aligning scope with available resources and leveraging feedback to improve project direction. I was able to make a more meaningful contribution to the field after shifting focus to a more tractable and under-explored problem. The skills and lessons from this experience are directly transferable to professional engineering practice, including managing uncertainty, adjusting technical scope, and maintaining progress under constraints.

10 References

- [1] D. Pujara, S. Sharma, and S. Chakrabarty, "Historical and planned uses of antenna technology for space-borne microwave radiometers," *IEEE Antennas and Propagation Magazine*, vol. 53, no. 3, pp. 95-114, 2011.
- [2] Soil Moisture Monitoring. Agriculture Victoria, Victoria, Australia, 2017.
- [3] Zhang, Y and Kerle, N. Satellite remote sensing for near-real time data collection. *Geospatial information technology for emergency response*, 6:75–102, 2008.
- [4] M. Kebe, M. C. E. Yagoub, and R. E. Amaya, "A survey of phase shifters for microwave phased array systems," *International Journal of Circuit Theory and Applications*, 2024. [Online]. Available: <https://onlinelibrary.wiley.com/doi/abs/10.1002/cta.4298>
- [5] N. Boopalan, A. Ramasamy, F. Nagi, and A. Alkahtani, "Planar array failed element(s) radiation pattern correction: A comparison," *Applied Sciences*, vol. 11, p. 9234, 10 2021.
- [6] Q. Lingling, J. Tao, Q. Jiahui, and Y. Yuqi, "Evaluation of failed arrays pattern recovery based on genetic algorithm," in *2018 International Applied Computational Electromagnetics Society Symposium - China (ACES)*, 2018, pp. 1–3.
- [7] H. Munsif and I. Ullah, "Malfunctioning conformal phased array: Radiation pattern recovery with particle swarm optimisation," *IET Microwaves, Antennas & Propagation*, vol. 18, no. 9, pp. 654–666, 2024. [Online]. Available: <https://ietresearch.onlinelibrary.wiley.com/doi/abs/10.1049/mia2.12495>
- [8] Constantine A Balanis. *Antenna Theory: Analysis and Design*. Harper and Row, 1982.
- [9] S. Roy, "A phase correction technique based on spatial movements of antennas in real-time (s.m.a.r.t.) for designing self-adapting conformal array antennas," Ph.D. dissertation, 09 2017.
- [10] Eugene Hecht. *Optics*, Global Edition. Pearson Education, Limited, 5th edition, 2016.
- [11] J.-H. Tsai, F.-M. Lin, and H. Xiao, "Low RMS phase error 28 GHz 5-bit switch type phase shifter for 5G applications," *Electronics Letters*, vol. 54, no. 20, pp. 1184-1185, 2018.
- [12] W. Lim, X. Tang, and K. Mouthaan, "L-band 360° vector-sum phase shifter using COTS components," in *2012 Asia Pacific Microwave Conference Proceedings*, 2012: IEEE, pp. 100-102. 249
- [13] Anant Sharma, Ajay Kumar, and A. N. Bhattacharya. A ku-band 6-bit digital phase shifter MMIC for phased array antenna systems. In *2015 IEEE MTT-S International Microwave and RF Conference(IMaRC)*, pages 404–407, 2015. doi: 10.1109/IMaRC.2015.7411411.
- [14] A. Vilenskiy and M. Makurin, "Analog varactor phase shifter," *2017 Progress In Electromagnetics Research Symposium - Spring (PIERS)*, St. Petersburg, Russia, 2017, pp. 3820-3825, doi: 10.1109/PIERS.2017.8262425.
- [15] L. Wang et al., "Highly linear Ku-band SiGe PIN diode phase shifter in standard SiGe BiCMOS process," *IEEE Microwave and Wireless Components Letters*, vol. 20, no. 1, pp. 37-39, 2009.
- [16] J. G. Yang and K. Yang, "Ka-band 5-bit MMIC phase shifter using InGaAs PIN switching diodes," *IEEE Microwave and Wireless Components Letters*, vol. 21, no. 3, pp. 151-153, 2011.
- [17] C.-E. Guan and H. Kanaya, "360 Phase Shifter Design Using Dual-Branch Switching Network," *IEEE Microwave and Wireless Components Letters*, vol. 28, no. 8, pp. 675-677, 2018.

- [18] Daniel Müller, S. Reiss, Hermann Massler, Axel Tessmann, A. Leuther, Thomas Zwick, and Ingmar Kallfass. A h-band reflective-type phase shifter MMIC for ism-band applications. pages 1–4, 06 2014.
- [19] J.-C. Wu, T.-Y. Chin, S.-F. Chang, and C.-C. Chang, "2.45-GHz CMOS reflection-type phase-shifter MMICs with minimal loss variation over quadrants of phase-shift range," *IEEE Transactions on Microwave Theory and Techniques*, vol. 56, no. 10, pp. 2180-2189, 2008.
- [20] K. T. Trinh, J. Feng, S. H. Shehab, and N. C. Karmakar, "1.4 GHz Low-Cost PIN Diode Phase Shifter for L-Band Radiometer Antenna," *IEEE Access*, vol. 7, pp. 95274-95284, 2019.
- [21] C.-S. Lin, S.-F. Chang, C.-C. Chang, and Y.-H. Shu, "Design of a reflection-type phase shifter with wide relative phase shift and constant insertion loss," *IEEE Transactions on Microwave Theory and Techniques*, vol. 55, no. 9, pp. 1862-1868, 2007.
- [22] M. Teshiba, R. Leeuwen, G. Sakamoto, and Terry Cisco. A SiGe MMIC 6-bit pin diode phase shifter. *Microwave and Wireless Components Letters*, IEEE, 12:500 – 501, 01 2003. doi: 10.1109/LMWC.2002.805534.
- [23] Hannes Venter and Tinus Stander. Phase shifters with multiple independently controllable bands utilising frequency-selective variable gain networks. *IET Microwaves Antennas Propagation*, 15:143–153, 01 2021.
- [24] I. Kalyoncu, E. Ozeren, A. Burak, O. Ceylan, and Y. Gurbuz, "A phase-calibration method for vector-sum phase shifters using a self-generated LUT," *IEEE Transactions on Circuits and Systems I: Regular Papers*, vol. 66, no. 4, pp. 1632-1642, 2019.
- [25] H. Munsif, B. D. Braaten, and Irfanullah, *Element Failure Correction Techniques for Phased Array Antennas in Future Terahertz Communication Systems*. Singapore: Springer Singapore, 2021, pp. 19–46. [Online]. Available: https://doi.org/10.1007/978-981-16-5731-3_2
- [26] Q. Lingling, J. Tao, Q. Jiahui, and Y. Yuqi, "Evaluation of failed arrays pattern recovery based on genetic algorithm," in *2018 International Applied Computational Electromagnetics Society Symposium - China (ACES)*, 2018, pp. 1–3.
- [27] O. P. Acharya and A. Patnaik, "Antenna array failure correction [antenna applications corner]," *IEEE Antennas and Propagation Magazine*, vol. 59, no. 6, pp. 106–115, 2017
- [28] B. Tang, J. Zhou, B. Tang, Y. Wang, and L. Kang, "Adaptive correction for radiation patterns of deformed phased array antenna," *IEEE Access*, vol. 8, pp. 5416–5427, 2020.
- [29] P. Zhou, Z. Zhang, and M. He, "Radiation pattern recovery of the impaired-radome-enclosed antenna array," *IEEE Antennas and Wireless Propagation Letters*, vol. 19, no. 9, pp. 1639–1643, 2020.
- [30] Raja Aasim Bin Saleem, Arslan Ali Shah, Hina Munsif, Ali Imram Najam, Shahid Khattak, and Irfanullah, "Pattern Compensation of a Planar Phased Array with Centre Elements Phase Malfunctioning Using a Genetic Algorithm," *Progress In Electromagnetics Research Letters*, Vol. 122, 21-28, 2024. doi:10.2528/PIERL24041404
- [31] N. Boopalan, A. K. Ramasamy, F. Nagi, and A. A. Alkahtani, "Planar array failed element(s) radiation pattern correction: A comparison," *Applied Sciences*, vol. 11, no. 19, 2021. [Online]. Available: <https://www.mdpi.com/2076-3417/11/19/9234>
- [32] M. Juneja and S. K. Nagar, "Particle swarm optimization algorithm and its parameters: A review," *2016 International Conference on Control, Computing, Communication and Materials (ICCCCM)*, Allahbad, India, 2016, pp. 1-5, doi: 10.1109/ICCCCM.2016.7918233.

- [33] F. Shigeki, "Waveguide Line (in Japanese)," Japan Patent Patent 06-053, 1994.
- [34] Maurizio Bozzi. Substrate integrated waveguide (SIW): An emerging technology for wireless systems. In 2012 Asia Pacific Microwave Conference Proceedings, pages 788–790, 2012. doi: 10.1109/APMC.2012.6421736.

11 Appendices

11.1 Appendix A: Project Risk Assessment

62935		RISK DESCRIPTION		STATUS	TREND	CURRENT	RESIDUAL		
RISK TYPE									
1. Activity or Task Based Risk Assessment									
RISK OWNER		RISK IDENTIFIED ON		LAST REVIEWED ON		NEXT SCHEDULED REVIEW			
Alexander Li		30/08/2024		01/09/2024		01/09/2027			
RISK FACTOR(S)	EXISTING CONTROL(S)	CURRENT	PROPOSED CONTROL(S)	TREATMENT OWNER	DUUE DATE	RESIDUAL			
The non-ionizing radiation hazard associated with this project primarily stems from the electromagnetic waves emitted by the antenna system, particularly in the high-frequency Ku and Ka bands. Extremely prolonged or intense exposure to these frequencies can potentially cause minuscule thermal effects, such as tissue heating.	Control: The testing will be conducted in a mostly enclosed anechoic chamber, and the experimenter will be on the outside, safe from the electromagnetic radiation Control Effectiveness:	Low							
Handling high-frequency RF components and power supplies may expose people to electrical shocks or burns, especially during testing and assembly.	Control: The equipments are grounded so that in the case of an internal short to the case, the case is not live. Control Effectiveness: Control: Induction of equipment usage, emphasising to always inspect equipment to check for any cable damages or exposed internal electronics before turning on, and if any issue is found, report to supervisor. Control Effectiveness:	Low							
Slips and trips hazards can arise from loose cables, tools,	Control: Maintaining a tidy lab environment and securing	Low							

	and equipment scattered on the floor during the assembly and testing of the antenna system. These obstructions can lead to accidents, especially in a cluttered workspace.	cables can significantly reduce the risk of slips and trips. Control Effectiveness: Control: Have induction to point out the likely causes of trips such as cluttered cables, and instructing the experimenter to always pay attention to the floor, can reduce the likelihood of slips and trips. Control Effectiveness:		
	The hazard of being struck by objects in this project arises from the potential for falling tools, equipment, or antenna components during assembly, testing, or adjustments. Unstable setups or improperly secured items can also pose a risk, such as unsecured door to the anechoic chamber.	Control: Have induction to explain the risks of protruding and unsecure objects, and instructing the experimenter to always make sure equipment is secured and away from the edge of tables, will reduce the likelihood of objects falling and protruding to cause damage. Control Effectiveness: Control: Wearing fully covering clothes can reduce scraping due to falling or protruding objects, reducing the severity of the risk. Wearing steel cap boots can reduce the damage caused by falling heavy equipment, like network analysers and signal generators. Control Effectiveness:	Low	
	Prolonged or repetitive awkward positions or movements, such as bending over workstations, or fine-tuning antenna fixtures in the anechoic chamber, could cause musculoskeletal stress. These activities can strain muscles, joints, and tendons, potentially leading to discomfort or injuries like back	Control: Instructing the experimenter to implement ergonomic practices and taking regular breaks, and using proper bending techniques can help mitigate these risks. Control Effectiveness:	Low	

powered by riskware.com.au

commercial in confidence

pain or repetitive strain injuries.			
Soldering involves working with heated soldering irons that can reach temperatures above 300°C, posing a significant burn risk. Accidental contact with the soldering iron or molten solder can result in severe skin burns.	Control: Student must be trained to handle the soldering iron with great control. The soldering will also be done under supervision by PhD students that share the lab. Control Effectiveness: Control: Wearing gloves and clothes that cover the arms can reduce the damage done by the soldering iron in the event that the iron approaches the skin. Control Effectiveness:	Low	
During soldering, the flux and solder materials release fumes that may contain harmful substances like lead, rosin, and other volatile organic compounds (VOCs). Inhalation of these fumes can lead to respiratory irritation, headaches, and potentially long-term health issues	Control: Using a fume extractor can ensure the fumes do not reach the student to be inhaled, reducing the likelihood and damage done by inhaling fumes. Control Effectiveness:	Low	

11.2 Appendix B: Risk Management Plan

This section is concerned with the non-OHS risk management plan, primarily related to the risks that threaten the successful completion of this project, and the risks that the completion of this project may have on the health, safety, commercial, political, environmental situations of society at large.

11.2.1 Major Activities

The first phase, Experimental Practice (2 weeks), will focus on gaining hands-on experience with antenna testing using an L-band phased array antenna. This foundational practice is crucial, as it directly informs the next step. Design and Simulation (7 weeks) will follow, where a new tri-band antenna will be designed, exploring various geometric parameters while running electromagnetic simulations to assess beamforming performance and cross-band interference. This phase is heavily dependent on the skills developed during the experimental practice, and is arguably the most important - since most of the intuitions of how the rest of the project will evolve will be developed here, informing how the rest of the project will be conducted.

Once the design and simulations are finalized, Fabrication and Beamforming Algorithm Development (3 weeks) will commence. During this time, the antenna will be sent for fabrication and the development of a beamforming algorithm will commence. This phase relies on the completion of the previous design and simulation tasks. Upon receiving the fabricated antenna, the Integration (3 weeks) phase will begin, where the antenna will be combined with the beamforming algorithm to prepare for testing. Finally, Testing and Data Collection (3 weeks) will take place in an anechoic chamber, followed by Analysis (3 weeks), where the results will be interpreted and areas for potential improvement will be identified.

The hazards and risks associated with each activity and their mitigation strategies are shown in Table 7.1.

11.2.2 Health Concerns

The L, Ku and Ka bands are microwave radiation. Prolonged exposure to high intensities leads to tissue heating. However, the most likely operation of the satellite that would use this technology is to sweep across a large area of land without much lingering at any particular spot. As a result, prolonged exposure is unlikely for any individual.

11.2.3 Public Concerns

Communication interference is a concern in the L frequency band due to the high demand for these frequencies by various critical services, such as GPS, satellite communications, and 5G networks. Interference can degrade signal quality and lead to data loss. To mitigate these risks, the directional beamforming investigated in this project, filtering, adherence to regulatory guidelines on transmission power, and error correction techniques, can minimize the potential for interference and ensure other services operating in this range aren't disrupted.

11.2.4 Risk Assessments

Non-OHS related risks are presented in Table 6.

Table 6 - Non-OHS related risk assessment

Project Risk	Risk	Likelihood	Consequence	Risk level	Mitigation	Residual Risk
Errors in Testing Practice	Incorrect measurements or mishandling of the L band antenna during practice	Possible	Minor	M	Ask detailed questions on procedures, double check setups, consult with experienced PhD students in the lab.	Low; PhD students not relevant to the project may be clueless. PhD student relevant to the project may be too busy. Will consult supervisor.
Inadequate Research	Significant gaps in RF design practices, leading to erroneous designs in the antennae, phase shifters, and tri-band integration that won't work and weeks of delays on the testing phases of the project	Possible	Disastrous	S	Ensure that all key areas of RF design related to phased array antennae are thoroughly understood. Revise the fundamentals. Consult supervisor and experienced PhD students for design review.	None of the consultants provide feedback, or are careless in the design review. Low likelihood of happening; be resourceful and seek help elsewhere, such as friends with RF knowledge.
Simulation Inaccuracies	Errors in electromagnetic simulations causing incorrect predictions of antenna behavior. More likely to result from misuse of simulation software.	Unlikely	Minor	L	Validate simulation results with simplified analytical models and cross-check with different simulation software.	No analytical knowledge exists regarding this particular design.
Fabrication Errors	Manufacturing defects such as deformed trace or missing components or errors during antenna assembly.	Unlikely	Serious	M	Identify these errors ASAP and send enquiries to manufacturer to remedy the problems.	It takes too long to wait for another antenna. Unlikely, considering the time available during summer holiday.
Misinterpretation of Data	Incorrect analysis of test data leading to false conclusions about antenna performance. Misguided recommendations for improvement, potentially leading to flawed designs in the future.	Possible	Serious	M	Cross-verify data interpretation with peers, use established analytical methods, and consider external validation.	Despite thorough cross-verification with peers, there is still a chance that subtle errors in data analysis could go unnoticed. Low likelihood that significant errors will be unnoticed, however.

11.3 Appendix C: Sustainability Plan

To incorporate sustainability into engineering is to design solutions and conduct engineering practices to meet the current project needs while not compromising future generations to meet theirs. This involves balancing environmental, social, and economic factors, summarised as the triple bottom line: people, planet, and profit. This project, which involves the development of a phased array antenna for soil moisture remote sensing, sustainable engineering plays a central role. By aligning with the United Nations Sustainable Development Goal (SDG) 6: Clean Water and Sanitation, the project aims to improve global water resource management through innovative technology.

11.3.1 SDG 6: Clean Water and Sanitation

SDG 6 focuses on "ensuring availability and sustainable management of water and sanitation for all." A key target under this goal is Target 6.4, which emphasizes increasing water-use efficiency and reducing water scarcity. Soil moisture data is essential for managing water use in agriculture, which consumes approximately 70% of freshwater globally [1]. By providing high-resolution, multi-frequency soil moisture data, this project will support more efficient irrigation practices, which in turn contributes to sustainable water management.

11.3.2 Stakeholders

Key stakeholders in this project include farmers, environmental agencies, the Australian Research Council, and governmental bodies responsible for water management. The effects of this project on them will be addressed in following sections.

11.3.3 Positive Environmental Impact

The primary environmental benefit of this project is its contribution to sustainable water management. By providing real-time soil moisture data, the technology helps prevent over-extraction from local water sources and improves irrigation efficiency. Additionally, the data enables better planning for climate change adaptation, as it helps predict floods and droughts, allowing communities to mitigate the effects of extreme weather events.

11.3.4 Negative Environmental Impact and Mitigation

Although satellite systems can have significant environmental impacts due to resource-intensive manufacturing and space debris at the end of their life cycle, this project aims to reduce its footprint by focusing on efficient design. By using energy-efficient methods for digital phase shifting instead of mechanical steering, the energy consumption of the system is minimized, reducing its overall environmental cost.

11.3.5 Resource Efficiency and Sustainable Design

The project's design includes a shared-aperture antenna system that operates across multiple frequency bands (L, Ku, and Ka), ensuring resource efficiency by using fewer materials and reducing the physical size of the hardware. The focus on passive sensing—which relies on naturally occurring signals—further reduces energy consumption compared to active systems, contributing to the sustainability of the design.

11.3.6 Social Impact

Enhanced soil moisture data has the potential to improve rural communities' quality of life by optimizing irrigation, increasing crop yields, and improving food security. Additionally, making this data accessible empowers farmers with the knowledge they need to make more informed decisions about water use.

11.3.7 Economic Impact

Economically, the project will help reduce operational costs in agriculture by increasing efficiency of water usage with the soil moisture information. This satellite-based remote sensing system provides continuous coverage at lower costs. The multi-band beamforming system offers more reliable data, benefiting other sectors such as disaster management, urban planning, and environmental conservation.

11.3.8 Summary

This phased array antenna project aligns with SDG 6 by contributing to more effective water resource management. Through the careful balance of environmental, social, and economic factors, the project demonstrates sustainable engineering principles. By optimizing water use, minimizing environmental impact, and providing broad social and economic benefits, this project not only addresses current water management challenges but also contributes to the long-term sustainability of global water resources.

11.4 Appendix D: Generative AI Statement

Generative AI use in FYP A (ENG/FIT4701)

The responses to this form will need to be copied and put into an appendix in your Progress Report.

Email *

alii0024@student.monash.edu

Name *

Alexander Li

Are you part of a team? If you are please add your team mates names below, if not, please answer 'No'

No

Campus

Clayton

Malaysia

Host Department

- Chemical and Biological Engineering
- Civil Engineering
- Electrical and Computer Systems Engineering
- Materials Science Engineering
- Mechanical and Aerospace Engineering
- Software Engineering
- Robotics and Mechatronics Engineering

Supervisor

Nemai Karmakar

This project has been conducted using AI tools *

- In this project, there will be no use of generative artificial intelligence (AI). All content in relation to the assessment task has been produced by the authors.
- In this project, the following generative AI will be used for the purposes nominated in part 2. (Please note: any use of generative AI must be appropriately acknowledged - see Learn HQ)
- In this project, AI writing assistants (e.g., Grammarly, Writesonic, Quillbot, Microsoft Editor) will be the only form of Generative AI used.
- This project involves the development or authoring of Unique Generative AI, Unique operation of commercially available Generative AI OR Unique non-generative AI (Machine Learning, Artificial Neural Network, Logistic Regression, etc.)

Permissions

The use of Generative AI has been discussed with and approved by my academic supervisor. *

- Yes
- No